Chapter 14

Different Levels of Self-Sufficiency of the Velocity Sedimentation Method in the Study of Linear Macromolecules

Georges M. Pavlov

Abstract The general principles for the interpretation of the sedimentation velocity for linear macromolecules are discussed in combination with the characteristics obtained by other hydrodynamic methods. The several levels of self-sufficiency of the sedimentation velocity method are demonstrated. They include scaling correlation between velocity sedimentation coefficient s_0 and concentration coefficient $k_s = K_{sks}{s_0}^{bks}$, application of the sedimentation parameter β_s for molar mass estimation, and qualitative conformation zoning of linear macromolecules using the normalized double logarithmic plots ($k_s M_L$vs $[s]/M_L$). The last example of self-sufficiency of the method is the study of the concentration dependence of the sedimentation velocity in combination with continuous c(s) distribution using general scaling law model of Sedfit software. This model allows to establish the relationship $s_0 = K_s M^{bs}$ for flexible polymers and perform further gross conformational analysis and analysis of the molar mass distribution. It is shown that the K_s coefficient is strongly dependent on the polymer concentration.

Keywords Velocity sedimentation • Sedimentation coefficient • Sedfit • Sedimentation parameter • Molar mass • Scaling relations

14.1 Introduction

Apparently, molecular hydrodynamics goes back to Archimedes of Syracuse and his concept of buoyancy which characterizes the difference in density between a particle/body and the surrounding liquid in which this particle moves (contrast of densities). Already in the new times, Stokes has obtained a relationship between

---

G.M. Pavlov (✉)
Institute of Macromolecular Compounds, Russian Academy of Sciences, Bol'shoi prospect 31, St. Petersburg 199004, Russia

Department of Physics, St. Petersburg State University, 7-9, Universitetskaya nab., St. Petersburg 199034, Russia
e-mail: g.m.pavlov@spbu.ru; georges.pavlov@mail.ru

S. Uchiyama et al. (eds.), *Analytical Ultracentrifugation*,
DOI 10.1007/978-4-431-55985-6_14

the translational friction coefficient of a rigid sphere and its radius. In 1911 Svedberg and Estrup used the precipitation rate of colloidal particles in the Earth's gravitational field (with acceleration of 1 g) to assess their size. They obtained the following relation when the notion of the velocity sedimentation coefficient was not yet introduced:

$$r_h = \left[(9/2)\,(uh)/\,(d - d)\,g'\right]^{1/2} = \Big[\,(9/2)\,(s\eta\overline{\upsilon}/\,(1 - \overline{\upsilon}\;\rho_0)\big]^{1/2} \tag{14.1}$$

The left side of the relationship (14.1) is the original one, and the right side is its modern paraphrase.

Here r_h is the hydrodynamic radius of the particle, η is the medium viscosity, $\delta \equiv \rho_0$ is the density of the solvent, $d = 1/\overline{\upsilon}$ is the density of the particle, $\overline{\upsilon}$ is the partial specific volume, and $u/g' \equiv s$ is the sedimentation coefficient according to the definition given later by Svedberg.

Conspicuously, in 1913, Dumanskiy, Jabotinsky, and Evseev (see also Introduction by T. Svedberg in Svedberg and Pedersen (1940)) were the first to use a *centrifuge*. They studied the precipitation rate of colloidal particles at $n = 2000$ rpm ($\approx$300 g) to measure particle sizes using the same relationships (14.1) which they have derived from the Stokes law. In 1913–1926, Svedberg and his coworkers have performed an enormous amount of creative and constructive work to design and build the *ultracentrifuge* which allows to achieve the fields of $\approx$ 200 000 g. On May 19, 1927, Svedberg gave his Nobel lecture entitled “The ultracentrifuge” (Svedberg 1927). Thus, a new scientific direction has emerged in molecular biophysics and nascent polymer science – analytical ultracentrifugation. In fact, Svedberg's lecture predicted the widespread use of analytical ultracentrifugation in future studies of various dispersed systems. Further results of the analytical ultracentrifugation obtained before the 1940s were summarized in the book (Svedberg and Pedersen 1940), which so far has not lost its value. The first investigations conducted by Svedberg himself were devoted to studying velocity sedimentation of globular proteins from different organic sources (e.g., Svedberg and Faehraeus 1926; Svedberg and Sjoegren 1928). These data represent an extensive library of velocity sedimentation coefficients of proteins and are given in a special chapter (Pedersen in the monograph Svedberg and Pedersen 1940). In a short while, the investigations of cellulose and its derivatives as well as the synthetic polymers were started (e.g., Stamm (1930); Singer and Gross (1934a, b); Kraemers and Nichols (1940)). In the mid-1950s, the study of DNA properties by AUC also began (see Peacocke and Schachman (1954), Kawade and Watanabe (1956)).

Currently, analytical ultracentrifugation methods are widely used in biophysics, polymer science, nanoscience, colloid science, and other related areas (Munk 1991; Schuster and Laue 1994; Laue and Stafford 1999; Lebowitz et al. 2002; Scott et al. 2005; Maechtle and Boerger 2006). Analytical ultracentrifugation has some experimental variations, and the most important and used among them are sedimentation velocity and sedimentation equilibrium (Schachman 1959; Fujita 1975). In this part, we will consider only the application of the first method.

In 1997 Beckman Instruments, Inc. (Palo Alto, USA) launched a new analytical ultracentrifuge. The progress made by Beckman Instruments in XLA/I model involves various aspects: up-to-date electrical drive, convenient temperature control of the apparatus, the development of optical detection systems, digital camera, and the online digitization of the measuring data. Since the XLI ultracentrifuge is equipped with two kinds of optics (the UV/Vis absorption detector and the Rayleigh interferometer), it became possible to use the new analytical ultracentrifuge to study a wide range of polymer molecules, both synthetic and natural.

The impressive breakthrough was made with the development of a commercial fluorescence detection system (FDS) for the analytical ultracentrifuge which has significantly extended the sensitivity of the boundary registration going up to picomolar concentrations of labeled solutes (MacGregor et al. 2004; Kroe and Laue 2009). The only problem left is incorporation of the corresponding tags into macromolecules; then it would be virtually possible to follow the sedimentation of individual macromolecule. (It will be indeed gold "nuts and bolts.")

After development of the XLA/I ultracentrifuge, the amount of information obtained in the course of one sedimentation velocity experiment (i.e., number of scans) increased by several orders of magnitude. This change necessitated development of software for processing raw data, and these softwares have been worked out by different teams of researchers. Pioneering works in this area were made by Stafford (1992, 2000) and Stafford and Braswell (2004); he elaborated the time derivative method dc/dt which is used in the Sedanal sedimentation velocity module. Several other methods have been developed for direct fitting of the sedimentation boundary; these methods are based both on approximate (Philo 1994; Behlke and Ristau 1997) and numerical (Schuck 1998; Demeler and Saber 1998) solutions of the Lamm equation. In these approaches, the diffusion process is directly taken into account. As a result, the distribution of sedimentation coefficients for the sample may be obtained, which in turn can be converted into the molar mass distribution. These software programs provide significant opportunities for extracting information from the impressive files of raw data obtained in the sedimentation velocity experiments by now.

The methods of molecular hydrodynamics are among the basic methods in polymer science and molecular biophysics (Tanford 1961; Volkenshtein 1963; Tsvetkov et al. 1970; Cantor and Schimmel 1980; Fujita 1990). The information obtained by these methods is essential for understanding the structure and gross conformation of isolated macromolecules. Namely, these methods are useful for estimating the size and shape of the individual macromolecules, for judging how quick the chain is coiled; in other words, they help to understand the degree of rigidity or flexibility of macromolecules and get the information about the intrinsic nonideality of the chain state (i.e., strength of the long-range intrachain interactions).

This contribution considers the ways of the analysis of the results obtained in the study of individual linear synthetic and natural macromolecules using the hydrodynamic methods, especially velocity sedimentation. The main experimental studies of linear chain molecules have been carried out during the second half of the twentieth century, but these studies are currently being continued with the aid of the modern analytical ultracentrifuge which is, however, now called "ProteomeLabTH XL-I Protein Characterization System" (strange nickname for the ultracentrifuge).

14.2 Essential Concepts of Molecular Hydrodynamics and Parameters Characterizing the Conformation of Linear Polymers

The linear chain *macromolecules contract into a coil* due to free or hindered rotation around valence bonds between atoms which form the backbone. However, the self-crossing configurations should be excluded from the consideration, i.e., *intrachain volume effects* should be taken into account. The *intrachain volume effects* lead to an increase in the chain size and also to changes of the chain size distribution function. In a weakly coiled chains, the *effects of intramolecular draining* are present, i.e., the flow of solvent molecules through a loose polymer coil is observed. This phenomenon leads to an increase in friction loss of the macromolecule moving in solution. The effects of the hydrodynamic interactions should be taken into consideration for the polymer coils moving in the solution. This interaction occurs not only between different macromolecules (*inter*coil interaction or concentration effects) but also within individual macromolecule (*intra*molecular interaction). The *intrachain hydrodynamic interaction* means that the moving chain element drags the solvent with it. The solvent is considered as a structureless continuum. The velocity of the adjacent solvent decreases proportionally to the distance from the chain element causing the flow. Other elements of the same chain involved in this velocity field are addicted by the driving fluid (solvent). These intrachain hydrodynamic interactions between the elements of the same chain in a moving liquid are described by the Oseen hydrodynamic tensor (Tanford 1961; Yamakawa 1971; Tsvetkov 1989; Doi 1996; Teraoka 2002; Rubinstein and Colby 2003).

A linear polymer macromolecule is characterized by its molar mass (M), contour length (L), mean-square end-to-end distance ($<h^2>$), or mean-square radius of gyration ($<R_g{}^2>$) (Tanford 1961; Tsvetkov et al. 1970); see Fig. 14.1. In the Gaussian coil limit, i.e., for the chains in the absence of intrachain excluded volume effects, $<h^2>$ and $<R_g{}^2>$ are related in a simple way: $<h^2> = 6<R_g{}^2>$. It is worth to mention that this relation is an exact result in the absence of excluded volume, but it also holds, in a proper approximation, for good solvents.

Hydrodynamic diameter (d), persistence length (a), or the Kuhn segment length (A = 2a), and mass per unit length ($M_L = M/L$), are the parameters being common for a homologous series of linear polymers which differs only by the contour lengths. For a homologous series of linear polymers, the mean-square end-to-end distance ($<h^2>$) and the mean-square radius of gyration ($<R_g{}^2>$) are related across the whole range of molar masses to the ratio of the contour length (L) to the

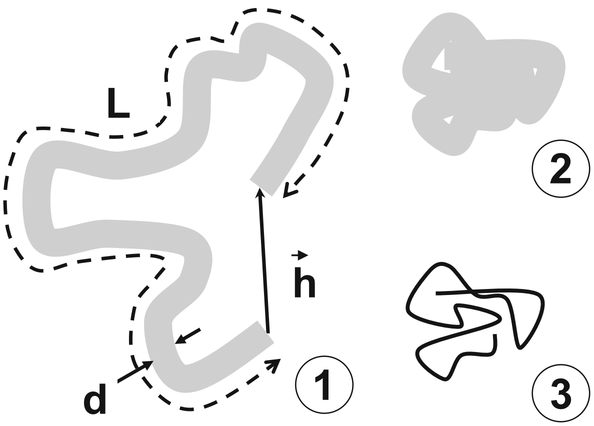

Fig. 14.1 Images of three coils having similar contour lengths ($L_1 = L_2 = L_3$) but different diameters *d* (1–3) and folded in varying degrees. These coils are characterized by the different statistical segment lengths (*A*: $A_1 > A_2 = A_3$), different diameters (*d*: $d_1 = d_2 > d_3$), different thermodynamic qualities of the solvent ($\varepsilon_1 > 0$, $\varepsilon_2 = \varepsilon_3 = 0$), and different intracoil draining effects (drained (1), non-drained (2), and partially drained (3) coils)

persistence length (a) by the following relationships (Kratky and Porod 1949; Benoit and Doty 1953; Landau and Lifschitz 1963):

$$< h^2 >= LA\ \left[1 - \left(1 - e^{-x}\right)/x\right], \tag{14.2}$$

$$< {R_g}^2 >= a^2\left\{(x/3) - [1-(2/x)\,[1-\ ((1-e^{-x})\,/x)]]\right\} \tag{14.3}$$

where x = L/a = 2 L/A is the reduced chain length.

The wormlike chain describes the behavior of chain molecules with the L/a values varying from very low to very high ones. For large (L/a) values, the wormlike chain has a Gaussian coil conformation. From this viewpoint, the wormlike chain is a more general model.

14.3 Relationships Between the Experimental Hydrodynamic Values and the Macromolecular Characteristics

The main characteristics obtained by the methods of molecular hydrodynamics are the velocity sedimentation coefficient s_0, the Gralen concentration coefficient k_s, the translational diffusion coefficient D_0, as well as the intrinsic viscosity [η]. All the experimental values should be obtained in the limit of infinite dilution.

Different experimental measurements can be expressed as intrinsic values ($[\eta]$, $[D]$, $[s]$, k_s) which are independent of the solvent properties at a first approximation. Each of these hydrodynamic characteristics is related to common macromolecular characteristics, which are, in the case of linear polymers, M and $< h^2 >$ (Svedberg and Pedersen 1940; Flory 1953; Tanford 1961; Tsvetkov et al. 1970; Yamakawa 1971; Cantor and Schimmel 1980; Pavlov and Frenkel 1986, 1988):

$$[\eta] = \varPhi < h^2 >^{3/2} / M, \tag{14.4}$$

$$[D] \equiv D_0 \eta_0 / T = k / \left(P < h^2 >^{1/2} \right), \tag{14.5}$$

$$[s] \equiv s_0 \eta_0 / \left(\Delta\rho / \Delta c \right) = M / P < h^2 >^{1/2} N_A \Big), \tag{14.6}$$

$$k_s = B < h^2 >^{3/2} / M, \tag{14.7}$$

where T is the absolute temperature, k is Boltzmann's constant, and N_A is Avogadro's number. The density increment ($\Delta\rho/\Delta c$) or buoyancy (Archimedes) factor ($1 - \overline{\upsilon}\, \rho_0$) is used to obtain a partial specific volume ($\overline{\upsilon}$), and ρ_0 is the solvent density. $\varPhi$ and P are the Flory hydrodynamic parameters; B is also a hydrodynamic dimensionless parameter. The values of $\varPhi = \varPhi$(L/A, d/A, ε) and $P = P$(L/A, d/A, ε) are functions of the relative contour length (L/A) and relative diameter (d/A), and parameter ε characterizes the thermodynamic quality of the solvent (or the long intrachain interactions). In the case of the absence of the excluded volume effects, when $\varepsilon = 0$, the values of $\varPhi = \varPhi$(L/A, d/A, $\varepsilon = 0$) and $P = P$(L/A, d/A, $\varepsilon = 0$) are tabulated in the frame of the wormlike cylinder theory (Yamakawa and Fujii 1973, 1974).

In the case of linear polymers of non-globular conformation, the sensitivity of the hydrodynamic characteristics to the changes in the molar mass decreases in the following order: Eq. (14.4) ≈ Eq. (14.7) > Eq. (14.5) > Eq. (14.6).

The comparison of Eqs. (14.5) and (14.6) immediately leads to the second Svedberg relationship, which is an essence of one of the absolute method of the molar mass determination, i.e., sedimentation-diffusion analysis:

$$M_{sD} = \left(RT / \left(1 - \overline{\upsilon}\, \rho_0 \right) \right) \left(s_0 / D_0 \right) = R\, [s] / aD \Big] \tag{14.8}$$

(The first Svedberg relationship is the relation (14.6).)

14.4 Degree of Solution Dilution

The use of [η], s_0, and D_0 requires extrapolation of the experimentally determined values to zero concentration of polymer *c*. In the vicinity of zero concentration, the following relationships (Tsvetkov et al. 1970; Yamakawa 1971) are applied:

$$\eta = \eta_0\left(1 + k_{1\eta}c + k_{2\eta}c^2 + \cdots\right) \; or \; \left((\eta/\eta_0)\ -1\right)/c = k_{1\eta} + k_{2\eta}c + \cdots \quad (14.9)$$

$$D = D_0\left(1 + (2A_2M - (k_s + \overline{\upsilon}))\,c + \cdots\right) \quad (14.10)$$

$$s^{-1} = {s_0}^{-1}\left(1 + (k_s + \overline{\upsilon})\,c + \cdots\right) \quad (14.11)$$

where η and η_0 are the dynamic viscosity of solution and solvent, A_2 is the second thermodynamic virial coefficient, and $k_{1\eta}$, $k_{2\eta}$, k_s are the concentration coefficients. All concentration coefficients in Eqs. (14.9, 14.10, and 14.11) contain molecular information. Two of them are very useful, namely, the *first viscosity concentration coefficient* $k_{1\eta} \equiv [\eta]$, the so-called intrinsic viscosity, and the concentration sedimentation coefficient k_s, the so-called Gralen coefficient.

In order to satisfy the linear regressions (14.9, 14.10, and 14.11) the solutions under study should belong to the zone of *dilute solutions*. This means that the neighboring coils in the solution must be spaced each other by a distance greater than their own size. The *degree of dilution* is usually characterized by dimensionless Debye parameter c[η] (c is polymer concentration expressed in $g \times cm^{-3}$, [η] is intrinsic viscosity expressed in $cm^3 \times g^{-1}$). The product of the intrinsic viscosity and the concentration of the solution represents a good approximation of the volume fraction ϕ of the polymer substance in solution, with $\phi = nv_1/V = mv_1$ $N_A/VM = c \times 0.36 < h^2 >^{3/2} \times N_A/M = (0.36N_A/\Phi)c[\eta] \approx c[\eta]$, where $v_1 = 0.36$ $< h^2 >^{3/2}$ is the volume occupied by the macromolecular coil in solution and m is the overall mass of the polymer dispersed in overall volume of solution V. The condition $c[\eta] = 1$ corresponds to the situation when each coil may contact with others, and the coils start to overlap. The dilute solution regime corresponds to the inequality $c[\eta] \ll 1$; the lower limit of concentration is determined by the sensitivity of the optical detection system used. Thus, the concentration of the solutions of linear macromolecules cannot characterize the degree of dilution of the solution. For example, the polymer solution with a concentration of ≈ 0.4 mg/ml $= 0.4 \times 10^{-3}$ g/cm^3 may be not diluted if the intrinsic viscosity [η] is higher than 2000 cm^3/g (for instance, this is the case for the high molar mass polystyrene Meyerhoff and Appelt (1979)).

Note that since the k_s value also characterizes the specific volume occupied by the macromolecule, the product k_sc will characterize the degree of dilution too. However, for the flexible chain polymers, the condition $k_sc < 1$ will be stronger than the condition $[\eta]c < 1$, as far as $k_s/[\eta] \approx 1.7$. Meanwhile, for the rigid-chain polymers, condition $k_s c < 1$ will overestimate the degree of dilution, because in this case $k_s/[\eta]$ is usually lower than 1.

14.5 Error of k_s Determination

The concentration range should be wide enough to obtain a reliable extrapolation to zero concentration, i.e., to make estimation of both values with good accuracy: intercept (s_0) and slope (k_s/s_0). We shall analyze the errors of determination of the s_0 and k_s values. The mean square errors were determined by the mean square linear approximation of the dependences $s^{-1} = f(c)$ following the relation (14.11). By way of example, let us consider the results obtained in the sedimentation study of chitosan and nitrate chitin solutions (Table 14.1 and Fig. 14.2) (Pavlov and Frenkel 1986). Obviously, the error of k_s value is larger because it includes the error of s_0 value and the error of the slope of the linear dependency (Eq. 14.11). The correlation between the relative errors of s_0 and k_s values is given in Fig. 14.2.

14.6 Scaling Relation Between k_s and $\underline{s_0}$

Since the publication of Newman and Eirich (1950) where k_s values were compared with the corresponding values of the intrinsic viscosity, attempts were made to determine the molecular meaning of the k_s coefficient. But in the first place, it was a matter of optimizing the study of the concentration dependence of sedimentation coefficient for a number of polymer-homologous series of fractions/samples, sometimes reaching up to 30–40. For this purpose, the direct comparison between s_0 and k_s represents the most advantageous way.

The comparison of k_s and s_0 allows establishing the cross-scaling relation between two experimental values (Pavlov and Frenkel 1982). Replacing the $< h^2 >$ value in the relation $k_s = B < h^2 >^{3/2}/\mathrm{M}$ with help of the Svedberg relation ($s_0 = (1- \overline{\upsilon}\ \rho_0) M/N_A P_0 \eta_0 < h^2 >^{1/2}$) allows to obtain the following relationship:

$$k_s = B\left((1-\overline{\upsilon}\rho_0)/N_A P_0 \eta_0\right)\left(M^2/{s_0}^3\right) \tag{14.12}$$

Using Kuhn-Mark-Houwink-Sakurada-type scaling relation ($s_0 = K_s M^{bs}$), the following correlation may be obtained:

$$k_s = \left((1-\overline{\upsilon}\rho_0)/N_A P_0 \eta_0\right)\left(B/{K_s}^{2/3}\right) {s_0}^{(2-3bs)/bs} = K_{kss} {s_0}^{\nu} \tag{14.13}$$

where $\nu \equiv \nu_1 = (2-3b_s)/b_s$.

Alternative scaling relations ($k_s \sim {s_0}^{\nu}$) can be obtained: $\nu_2 = (4-3b_s)/3b_s$ from the Peterson theory (1964) of straight cylinder sedimentation (see also Fujita et al.

Table 14.1 Some hydrodynamic characteristics, their relative errors, and molar masses of chitosan macromolecules in 0.33 m $CH_3COOH + 0.3$ m NaCl solution at 294K[a]

	$[\eta]$	$s_0 \times 10^{13}$	$(\Delta s_0/s_0) \times 10^2$	k_s	$(\Delta k_s/k_s) \times 10^2$	$M_{ks} \times 10^{-3}$	$(\Delta M/M_{ks}) \times 10^2$	$M_{sD} \times 10^{-3}$
N	cm^3g^{-1}	s		cm^3g^{-1}		g mol^{-1}		g mol^{-1}
1	840	2.4	3.8	470	9.8	175	11.2	183
2	790	2.4	0.5	415	1.2	165	8.4	178
3	580	2.35	1.3	420	3.8	155	8.8	148
4	740	2.3	2.2	470	5.5	165	9.4	186
5	740	2.3	0.5	510	2.0	165	8.4	172
6	460	2.2	1.8	450	4.9	150	9.1	113
7	370	2.15	0.5	260	2.3	105	8.5	73
8	360	2.05	2.4	220	13.6	95	11.4	106
9	305	1.9	5.3	270	18.5	95	14.8	82
10	340	1.9	4.2	270	15.9	95	13.2	83
11	440	1.9	2.6	230	13.0	90	11.3	74
12	370	1.8	1.7	240	7.9	80	9.6	80
13	295	1.8	2.8	210	11.4	80	11.0	86
14	310	1.7	2.9	220	12.7	70	11.4	64
15	240	1.65	4.2	200	13.0	60	12.4	55
16	100	1.35	3.7	150	16.7	45	13.1	27
17	170	1.3	3.1	70	28.6	25	17.2	38
18	45	1.0	8.0	60	80.0	16	42.6	14

[a] Chitosan was obtained from the krill that was caught off the coast of Kamchatka. Its degree of deacetylation was 0.80, which corresponds to the molar mass of the repeating unit of $M_0 = 169$. Chitosan fractions were investigated in the following buffer solvent: 0.33 M $CH_3COOH + 0.3$ M NaCl. In this solvent of high ionic strength, the polyelectrolyte effects are suppressed. This solvent was characterized by the density $\rho_0 = 1.015$ g/cm^3 and the viscosity $\eta_0 = 1.05$ mPa × s values at 294 K. Buoyancy factor was determined pycnometrically and was equal to $(1 - \upsilon\rho_0) = 0.38$ with a mean relative error of 4.7×10^{-2}. Velocity sedimentation of these fractions was investigated using the analytical ultracentrifuge MOM 3170 (Hungary) at a rotor speed of 40×10^3 rpm in a double-sector synthetic boundary cell; the height of the centerpiece was 12 mm (Pavlov and Selyunin 1986). The optical system of recording the sedimentation boundary was the Lebedev's polarizing interferometer (Tsvetkov et al. 1970)

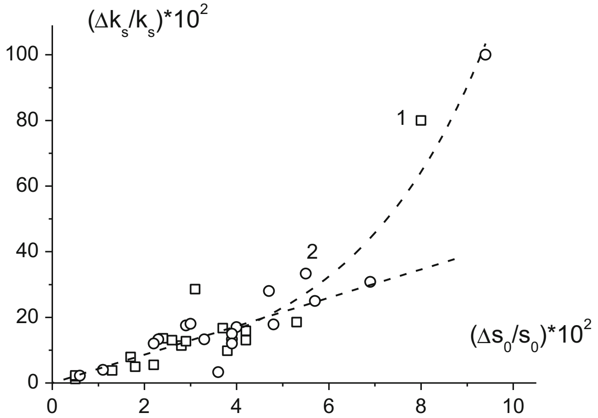

Fig. 14.2 Comparison of the relative errors of velocity sedimentation coefficient s_0 and Gralen coefficient k_s for the chitosan fractions studied in buffer solvent 0.33 M CH_3COOH + 0.3 M NaCl (*1*) and chitin nitrate fractions in dimethylformamide (*2*)

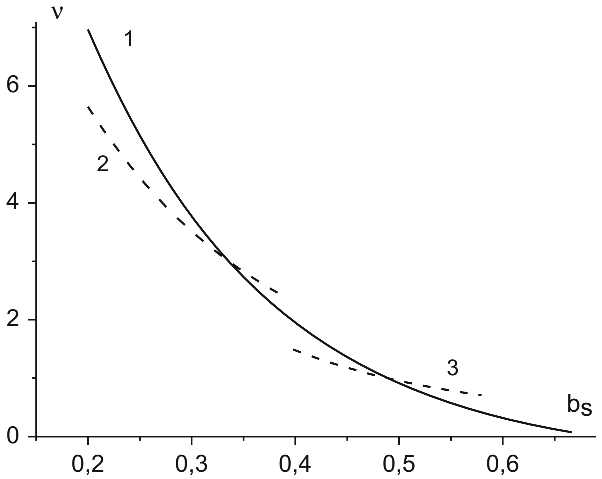

Fig. 14.3 Dependencies of the scaling coefficients ν on b_s: (*1*) $\nu \equiv \nu_1 = (2 - 3b_s)/b_s$ (Pavlov and Frenkel 1982); (*2*) $\nu_2 = (4 - 3b_s)/3b_s$ for the straight cylinder (Peterson 1964); and (*3*) $\nu_3 = (1 - b_s)/b_s$ for the coils under θ-conditions (Imai 1970; Freed 1983; Muthukumar and de Mense 1983)

1966) and $\nu_3 = (1 - b_s)/b_s$ for the random-coil macromolecules under θ-conditions (Imai 1970; Freed 1983; Muthukumar and de Mense 1983). Figure 14.3 shows the dependence of ν on b_s.

The values of ν_1 and ν_2 are close to each other in the range of $b_s < 0.3$ corresponding to rigid-chain macromolecules. At $b_s = 0.5$ (random coils under θ-conditions), we have $\nu_1 = \nu_3$. Consequently, the cross-scaling dependence

$$k_s = K_{kss} {s_0}^{(2-3bs)/bs} \tag{14.14}$$

has a general meaning and can be used for b_s value estimation for all spectrum of linear macromolecules.

Thus, the study of concentration dependence of sedimentation coefficient for three or four fractions in the possibly wide range of s_0 allows to establish the correlation given in Eq. 14.13 and to obtain a reliable estimation of the concentration coefficients k_s for other fractions of the studied series. Furthermore, the b_s value may be determined (Eq. 14.14); this is a key parameter in transformation of the sedimentation coefficient distribution of a sample into the molar mass distribution, as $ds_0/dM = b_s {K_s}^{1/bs} {s_0}^{(bs-1)/bs}$. The $\mathrm{b_s}$ value is also necessary for the application of the continuous c(s) model with general scaling law of Sedfit suite to treat the velocity sedimentation data.

It should be noted that the k_s values can vary within wide limits (from a few to several thousand of $\mathrm{cm^3/g}$) for the same homologous series of linear polymer systems. The k_s values are different for linear macromolecules of various conformational status and scale differently with s_0 values (Fig. 14.4). In the case of globular structures, the values of k_s vary slightly (≈(4–10) $\mathrm{cm^3/g}$) and are weakly dependent on the sedimentation coefficient (see Fig. 14.4 and Table 14.2). In the case of more rigid macromolecules, the more of them are draining, the greater are the values of k_s and the steeper is the dependence of k_s on s_0 (Fig. 14.4).

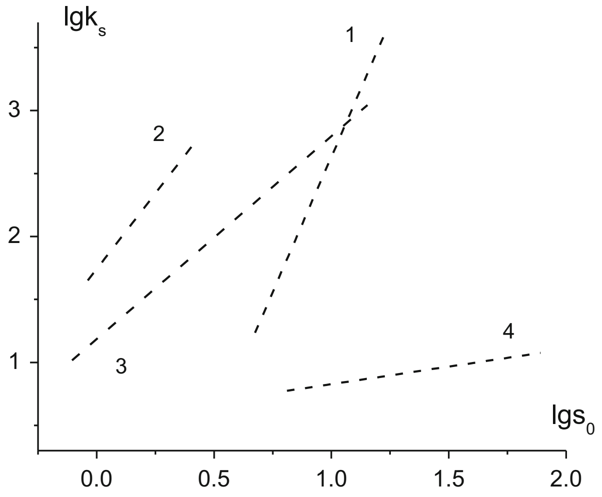

Fig. 14.4 Comparison of the dependencies k_s *vs.* s_0 in double logarithmic scale, characterizing different types of linear chain conformations: (*1*) extra-rigid (*Schizophyllum commune* polysaccharide), $k_s \sim {s_0}^{4.3\pm0.2}$ (Yanaki et al. 1980); (*2*) rigid (chitosan), $k_s \sim {s_0}^{2.4\pm0.2}$ (Pavlov and Selyunin 1986); (*3*) flexible (poly(1-vinyl-2-pyrrolidone)), $k_s \sim {s_0}^{1.61\pm0.07}$(Pavlov et al. 1990); and (*4*) globular (globular protein), $k_s \sim {s_0}^{0.25\pm0.07}$ (Creeth and Knight 1965)

Table 14.2 The limits of the scaling indices $\boldsymbol{b_s}$, $\boldsymbol{b_\eta}$, and $\boldsymbol{b_{kss}}$ values for different types of gross polymer conformations

Gross conformations	Types of polymer systems	b_s	b_η	b_{kss}
Globular/rigid sphere	Globular proteins, dendrimers, glycogen	$2/3 = 0.67$	≈ 0	≈ 0
Thick and relatively short macromolecules	Brushlike linear polymer	$0.5 < b_s < 0.67$	$0.5 \geq b_\eta > 0$	$1 > b_{kss} > 0$
Θ-condition	Flexible polymers	0.50	0.50	1
Rigid macromolecules without intrachain volume effect	Rigid macromolecules in the range of very high M	0.50	0.50	1
Thermodynamically good solvent, non-draining coil	Flexible polymers	$0.4 < b_s < 0.5$	$0.85 \geq b_\eta > 0.5$	$2 > b_{kss} > 1$
Rigid macromolecules, crankshaft conformation	Cellulose, cellulose derivatives, aromatic polyamides (moderate M range)	$0.33 < b_s < 0.5$	$1.0 \geq b_\eta > 0.5$	$3 > b_{kss} > 1$
Extra-rigid	Helical structures such as DNA, polysaccharides, schizophyllan, xanthan	$\cong 0.25 < b_s < 0.3$	$1.8 \geq b_\eta \geq 1$	$5 > b_{kss} > 3.7$

14.7 Scaling Relations Between Other Hydrodynamic Values and Molar Mass

To quote from Fujita (1990), "one of the most surprising generalities in the world of polymers is that $[\eta]$ for a series of homologous polymers under a fixed solvent condition follows a simple power law over an extended range of M." We can add that such relationships are also observed for all other hydrodynamic characteristics: s_0, k_s, and D_0 and between them; this was shown above for the $s_0 - k_s$ correlation. In principle, this kind of dependence is characteristic of fractal systems in which any part of the object is similar to the whole (de Gennes 1979; Mandelbrot 1982). The comparison of hydrodynamic characteristics with each other and with molar mass allows to obtain cross (among hydrodynamic characteristics) and canonic (among hydrodynamic characteristics and molecular mass) relationships of Kuhn-Mark-Houwink-Sakurada type or hydrodynamic scaling relationships. In general, they may be given as the following:

$$P_i = K_{ij} P_j^{\,bij} \tag{14.15}$$

where $\mathrm{P_i}$ is one of the hydrodynamic characteristics $[\eta]$, D_0, s_0, or k_s and P_j is another hydrodynamic characteristic from this array or molar mass. In the case of homologous series of linear polymers, the scaling indices $\mathrm{b_{ij}}$ are intercorrelated (Tsvetkov et al. 1970; Pavlov and Frenkel 1995) in the following ways: $b_{sD} = b_s/b_D$, $b_{D\eta} = b_D/b_\eta$, $b_{s\eta} = b_s/b_\eta$, $|b_D| = (1 + b_\eta)/3$, $|b_D| + b_s = 1$, and $b_{kss} = (2 - 3b_s)/b_s$, where the double underline index refers to cross-correlations and the single underline index refers to correlations of appropriate hydrodynamic characteristic with molar mass. (For instance, b_{sD} is the index of the power function between s_0 and D_0, which is represented as $s_0 = K_{sD} {D_0}^{bsD}$. b_s and b_D are the indices of the power functions between M and s_0 and between M and D_0, respectively: $s_0 = K_s M^{bs}$, $D_0 = K_D M^{bD}$.)

It is important to note that further molecular interpretation of the hydrodynamic characteristics will be the more accurate the wider is the molar mass range of investigated homologous series. At the same time, the $\mathrm{b_{ij}}$ value may vary in different ways during the transition *from very high to very low molar masses (contour lengths)* (Bloomfield 1968; Budtov 1992) (Fig. 14.5).

For any kind of linear macromolecules, there is a certain range of contour lengths where the coil maturation happens. Just in this range of the molar masses, the changes in the slopes of KMHS plots may be observed. The change of the slope in the KMHS plots is more easy to observe for $[\eta]$ dependence (b_η value) and less easy to see for the $\mathrm{s_0}$ dependence (b_s value), because $[\eta] \sim\ <h>^{3/2}$ and $s_0 \sim\ <h>^{-1/2}$, i.e., the value of $[\eta]$ is more sensitive to changes in the size and shape of the coil than the s_0 value.

The analyzed polymer can be referred to a certain class according to the type of the change in the respective slope. This is illustrated in Fig. 14.5a. The data obtained for polyvinylpyrrolidone (14.1) demonstrate a decrease in slope from $b_\eta = 0.74$ in

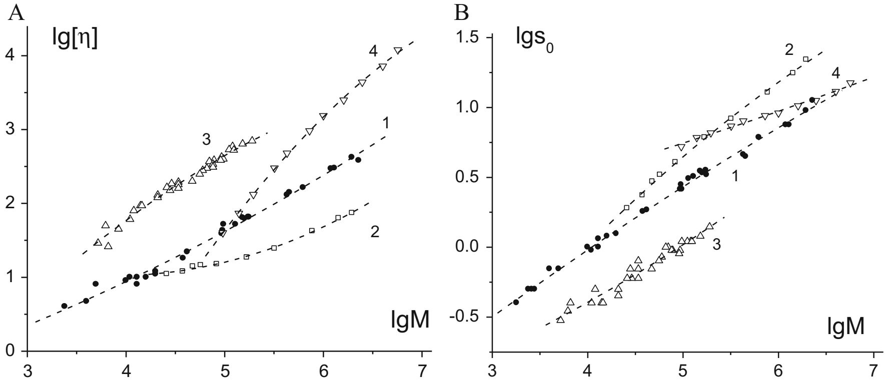

Fig. 14.5 Scaling plots of the hydrodynamic characteristics: (**a**) canonical Kuhn-Mark-Houwink-Sakurada (KMHS) plot $[\eta] = K_\eta M^{b\eta}$ and (**b**) dependencies of velocity sedimentation coefficient on the molar mass in double logarithmic scale or KMHS-type plot $s_0 = K_s M^{bs}$
The comparison of the linear macromolecules of different structures and equilibrium rigidity was made: flexible, poly(1-vinyl-2-pyrrolidone) (PVP) in 0.1 *M* sodium acetate solutions (*1*) (Pavlov et al. 1990); brushlike, styrene-methyl methacrylate brush copolymer in bromoform (*2*) (Magarik et al. 1978); rigid, poly(2,2′-p-phenylene-(5-benzimidazole)) isophthalamide (PBIA) in dimethylacetamide + 3%LiCl (*3*) (Pavlov and Selyunin 1986); and extra-rigid, the triple helix of *Schizophyllum commune* polysaccharide (schizophyllan) in water (*4*) (Yanaki et al. 1980)

the high molar mass region to $b_\eta \approx 0.50$ in the low molar mass region; this pattern corresponds to the behavior of flexible macromolecules in thermodynamically good solvents. Thus, in this case, the deviation of b_η value from 0.5 in the high molar mass region is attributed to the intrachain volume effects (intrinsic nonideality). System 2 in Fig. 14.5a represents a thick macromolecule which is characterized by a large transverse dimension. In this case, a decrease in the slope of the $[\eta]$ dependence *vs.* molar mass in the region of small contour lengths of the main chain is also observed. The b_η value can be significantly less than 0.5, which is explained by the comparability of longitudinal and transverse dimensions of the coil when the chain length is short enough. The systems 3 and 4 describe the behavior of the rigid polymer for which is characteristic the approaching of molecular conformation to slightly bending rod with decrease in chain contour length, and b_η becomes higher than 1. In this case, deviation of the b_η value from 0.5 is attributed to the effects of intramolecular draining associated with high equilibrium rigidity of the chains (high values of persistent length). The $[\eta]$ dependence *vs.* molar mass for rigid macromolecules is concave downward in the opposite direction as compared with that for flexible macromolecules which is concave upward (system 1). Figure 14.5b shows the dependence of s_0 *vs.* molar mass for the same systems. In this connection, two circumstances should be noted. First, the changes in the slopes of the curves shown in this figure are much weaker than the slope for the intrinsic viscosity values; second, these changes should show the opposite trend.

Table 14.2 gives the comparison between the b_s, b_η, and b_{kss} indexes for linear macromolecules with different conformational status. Comparison of variation of the b_η and b_{kss} indices with changing conformational type of the macromolecules shows that the direct comparison between the sedimentation coefficient s_0 and the Gralen coefficient k_s is more sensitive to conformational changes of macromolecules than the comparison between $[\eta]$ and M. This fact has led to the establishment of conformational zones of macromolecules considering the normalized plot of k_sM_L vs. $[s]/M_L$. It is one of the examples of self-sufficiency of the sedimentation velocity method in the conformational analysis of linear polymers (Pavlov and Frenkel 1986; Pavlov 1997).

14.8 Another Level of Self-Sufficiency of Velocity Sedimentation Data: Sedimentation Parameter and Hydrodynamic Invariant

Wales and van Holde (1954) were the first to suggest estimating molar masses of polymers from the experimental data obtained in the study of the concentration dependence of sedimentation velocity. As was shown by Wales and van Holde (1954), using the s_0 and k_s values, it is possible to estimate the molar mass of the flexible polymer chains by the following relation:

$$M = 4.85\pi N_A[s]^{3/2}{k_s}^{1/2} \tag{14.16}$$

A reexamination of this problem from the original theoretical standpoint was carried out later by Rowe (1977). The definitive result for the sedimentation of solvated molecules is given in the following equation:

$$M = N_A(6\pi)^{3/2}[s]^{3/2}\{(3\overline{\upsilon}/4\pi)\,[(k_s/2\overline{\upsilon}) - (\upsilon_s/)]\}^{1/2} \tag{14.17}$$

where v_s, according to Rowe, is the specific volume occupied by the sedimenting component (solute + entrained solvent + bound solvent). Rowe gave the following approximation for the $v_s/\overline{\upsilon}$ ratio:

$$\upsilon_s/\overline{\upsilon} = k'(k_s/\,[\eta])^{-1} \tag{14.18}$$

where k' is the Huggins parameter. For the majority of polymer systems, the second term in brackets in Eq. (14.17) is negligible as compared with the first one and is far lower than the error of k_s determination, so Eq. (14.17) can be rearranged as:

$$M \cong 9\pi N_A[s]^{3/2}{k_s}^{1/2} \tag{14.19}$$

Equations (14.16) and (14.19) differ only in numerical coefficients, and for some comparative purposes (e.g., scaling relation), they can give the same results.

The Wales-van Holde-Rowe Eqs. (14.16 and 14.19) were presented in general form with the introduction of the sedimentation parameter β_s (Pavlov and Frenkel 1986). In fact, this idea has been already implicitly contained in the paper of Wales and van Holde (1954). Actually, the sedimentation coefficients s_0 (first Svedberg equation) and k_s depend differently on molecular mass and size of macromolecules (Eqs. 14.6 and 14.7). The exclusion of $< h^2 >$ from Eqs. (14.6) and (14.7) allows to obtain the following expression:

$$\beta_s \equiv {B_s}^{1/3} {P_0}^{-1} = N_A \, [s] \, {k_s}^{1/3} M^{-2/3} \tag{14.20}$$

where β_s is the sedimentation parameter introduced by Pavlov and Frenkel (1986, 1988, 1995).

Obviously, the sedimentation parameter β_s is an analogue of the hydrodynamic invariant β (Mandelkern and Flory 1952).

The introduction of the sedimentation parameter was supported by the extensive set of experimental data available in the literature for linear uncharged polymers, both synthetic and natural. Analysis of almost entire data library on the velocity sedimentation of macromolecules indicates that the value of parameter β_s is practically invariant both in terms of molar mass and with respect to the structure of the repeating unit of the linear polymer (Pavlov and Frenkel 1995; Pavlov 1997). Table 14.3 lists the average experimental values of the sedimentation parameter β_s, parameter B_s for different polymer classes, and also classical hydrodynamic invariant $\beta \equiv A_0/k$.

The invariance of β_s value makes it possible to use Eq. 14.20 for determining molar mass of the polymer macromolecules using the data obtained only from

Table 14.3 Averaged experimental values of the sedimentation parameter β_s, hydrodynamic invariant β (and A_0), and parameter B_s

Polymer-solvent	${\beta_s}^a 10^{-7}$ mol$^{-1/3}$	$B_s 10^{-23}$ mol^{-1}	$\beta^{**} 10^{-7}$ mol$^{-1/3}$	${A_0}^b 10^{10}$
Flexible-chain polymers under θ-conditions	1.0	1.33	1.08	3.21
Flexible-chain polymers in thermodynamically good solvents.	1.25	2.61	1.08	3.21
Rigid-chain polymers	1.0	1.33	1.24	3.69
β1-4 glucanes and their derivatives	1.0	1.33	1.14	3.39
Globular proteins	1.17	2.14	1.01	3.00

[a] Mean-square errors are $\approx 6\,\%$, $P_0 = 5.11$

[b] $A_0 = k\beta$ – Mandelkern-Flory-Tsvetkov-Klenin hydrodynamic invariant, k is Boltzmann constant

Note that expressed in the same unit the both β and β_s values are close to each other (see Table 14.3, columns 2 and 4)

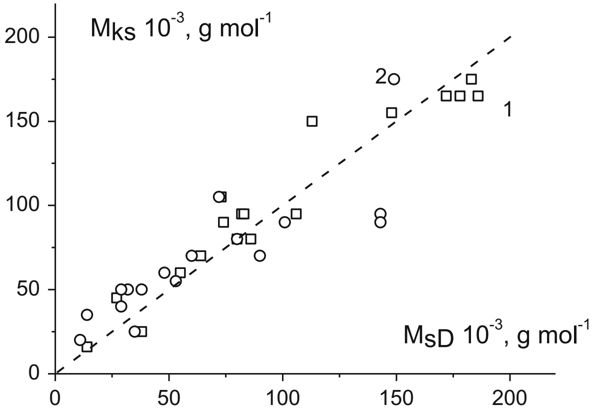

Fig. 14.6 Comparison of the molar mass values for chitosan (1) and chitin nitrate (2) calculated from the data of the sedimentation-diffusional analysis (M_{sD}) and from the s_0 and k_s values (M_{ks}, Eq. 14.21). Chitosan fractions were investigated in a buffer solvent: 0.33 M $CH_3COOH + 0.3$ M NaCl. Chitin nitrate fractions were investigated in dimethylformamide. *Dashed line* is drawn with a slope equal to 1

velocity sedimentation experiments:

$$M_{ks} = (N_A/\beta_s)^{3/2}[s]^{3/2}{k_s}^{1/2} \tag{14.21}$$

Good correlation is observed between independently measured M_{sD} values and those determined from the s_0 and k_s values. Figure 14.6 demonstrates this kind of correlation observed for fractions of chitosan and chitin nitrate.

Knowledge of the molar masses opens up the possibilities for further molecular interpretation of s_0 and k_s values. Useful applications of this concept have been demonstrated in various publications for different polymers (Tarabukina et al. 1991; Pavlov et al. 1995, 2003; Harding et al. 2011a; Morris and Harding 2013).

One of the definitions of Flory-Mandelkern-Tsvetkov-Klenin hydrodynamic invariant β (or $A_0 \equiv k\beta$) (Mandelkern and Flory 1952; Tsvetkov and Klenin 1953) is given by the following relation:

$$\beta \equiv \Phi^{1/3}P^{-1} = N_A\,[s]\,[\eta]^{1/3}M^{-2/3} \tag{14.22}$$

(Traditionally, in this case, the intrinsic viscosity is denominated in 100 cm^3/g.)

The ratios $\Phi^{1/3}/P$ and $B^{1/3}/P$ and thus A_0 and β_s are not strictly constant even theoretically (Table 14.4); they are experimentally found to be invariant (i.e., within the incertitude of the measurements) in the case of homologous polymers with different chain lengths. The theoretical values of the Flory hydrodynamic parameters P_0 and Φ_0 depend on the models and mathematical approximations. The limiting theoretical values of Φ and P for a Gaussian coil ($M \to \infty$), obtained after a preliminary averaging of the hydrodynamic Oseen's tensor, are $\Phi_0 = 2.87 \cdot 10^{23}$

Table 14.4 Theoretical values of Flory hydrodynamic parameters P_0, Φ_0, and hydrodynamic invariant $A_0 \equiv kP_0\Phi_0{}^{-1/3}$ (g cm^2 s^{-2} K^{-1} mol$^{-1/3}$) for polymer chains in the absence of intrachain excluded volume effects

P_0	Φ_0 10^{-23}mol^{-1}	A_0 10^{10}	References
(Sphere) 6π[a]	(Sphere) 2.5[a]	2.914	Tanford (1961)
7.35[b]	4.3	3.05	Kuhn et al. (1953) and Tsvetkov et al. (1970)
5.11[c]	3.62	4.15	Kirkwood and Riseman (1948)
5.11[c]	2.19	3.51	Hearst and Tagami (1965)
5.11[c]	2.86	3.84	Hearst and Stokmayer (1962) and Yamakawa and Fujii (1973, 1974)
5.99[d]	2.51	3.13	Zimm (1980) and de la Torre et al. (1982, 1984)
5.3[d]	1.9	3.23	Bernal et al. (1991)
6.20[e]	2.36	2.96	Oono (1985)

[a] For sphere $f_0 = 6\pi\eta_0 R$; $[\eta] = 2.5\,(4\pi/3)\,N_A\,(R^3/M)$

[b] Obtained with macroscopic models of polymer chains

[c] Obtained with preaveraging approximation of the tensor of the hydrodynamic interactions

[d] Obtained by Monte Carlo simulation without preaveraging approximation

[e] Obtained with renormalization groups theory

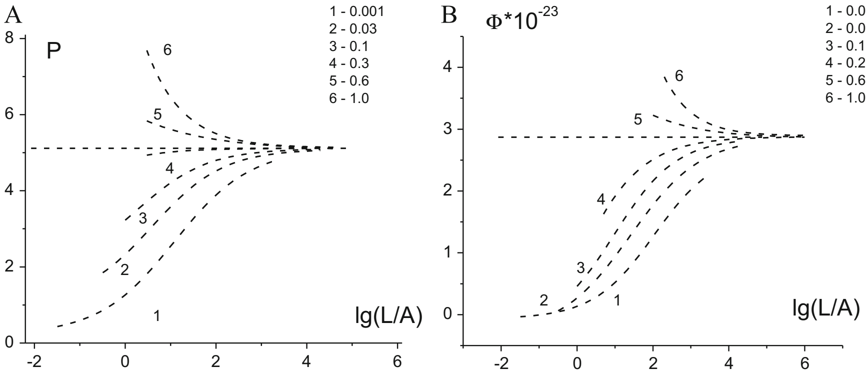

Fig. 14.7 The Flory parameters *P* (*A*) and *Φ* (*B*) as function of the relative contour length *L*/*A* of wormlike cylinder in semilogarithmic scale for different relative thickness *d*/*A* of cylinder from *d*/*A* = 0.001 up to *d*/*A* = 1 (Yamakawa and Fujii 1973, 1974)

and $P_0 = 5.11$ (Yamakawa 1971; Tsvetkov 1989, Fig. 14.7). They are affected by the preaveraging of the Oseen hydrodynamic tensor, as studied by the Monte Carlo simulation method (Zimm 1980; de la Torre et al. 1982, 1984; Bernal et al. 1991) and by renormalization group calculations (Oono 1985).

Thus, the basis of the similarity of two invariants is the same physical dimensions (cm^3/g); in other words, both $[\eta]$ and k_s are the functions of the specific volume of macromolecules. At the same time, Eqs. 14.20 and 14.22 expose the fundamental difference between β (or A_0) and β_s. This difference consists of the following. The value β is obtained from *M* and from two experimental values s_0 and $[\eta]$ which, in turn, are obtained in different kinds of experiments. In these experiments, a macromolecule performs different kinds of movement, namely, translational (s_0) and rotational ($[\eta]$). The sedimentation parameter β_s is obtained from M and two experimental values s_0 and k_s obtained in a single series of experiments where the macromolecule is studied under exactly the same translational conditions.

The calculation of the hydrodynamic invariants A_0 and β_s is a check for the mutual coherence of a set of the experimental data. These values should not go beyond a certain range of values indicated in Tables 14.3 and 14.4. Positioning of the A_0 and β_s values in these ranges allows further interpretation of the hydrodynamic characteristics. Otherwise, we need to analyze the causes of mismatch in the primary experimental data or to admit that the sizes of macromolecules are not equivalent in different types of movements.

14.9 Relationship Between Hydrodynamic Values and Conformational Parameters A and d in the Model of Wormlike Chain

In the limit of low molar mass chains ($L/A < 2.3$; $L \gg d$), a model of a weakly bending rod or a cylinder can be used that provides M_L and d through a linear regression (Broersma 1969; Yamakawa and Fujii 1973):

$$[s] = (M_L/3\pi N_A)\,[lnM - ln\,(M_L d) + 0.386) \qquad (14.23)$$

In principle, the slope of $[s] = f(lnM)$ in the range of lowest L/A values (<2) allows estimating linear density of the chain M_L. For this purpose, a sufficient number of experimental data in the corresponding range of molar masses should be available. However, these conditions are not frequently realized. The rare examples are the cases of extra-rigid macromolecules (Yanaki et al. 1980; Sato et al. 1984). The more flexible are the macromolecules, the lower molar mass samples must be studied (Fig. 14.8). This condition imposes significant restrictions on using velocity sedimentation data to obtain the M_L value.

A similar relationship was obtained for the intrinsic viscosity of slightly bending rods:

$$M^2/\,[\eta] = \left(45{M_L}^3/2\pi N_A\right)[lnM - ln\,(M_L d) - 0.697] \qquad (14.24)$$

It should be noted that the intrinsic viscosity data must be obtained in the region of smaller contour lengths (i.e., molar masses) than that used in velocity sedimentation experiments. This condition renders it more difficult to use intrinsic viscosity for determining the M_L value.

The dimensions of long linear chains are determined by two main factors: the short- and long-range interactions. The stronger is the short-range interaction, the stiffer is the chain; therefore, the coil becomes spongy, i.e., permeable for solvent

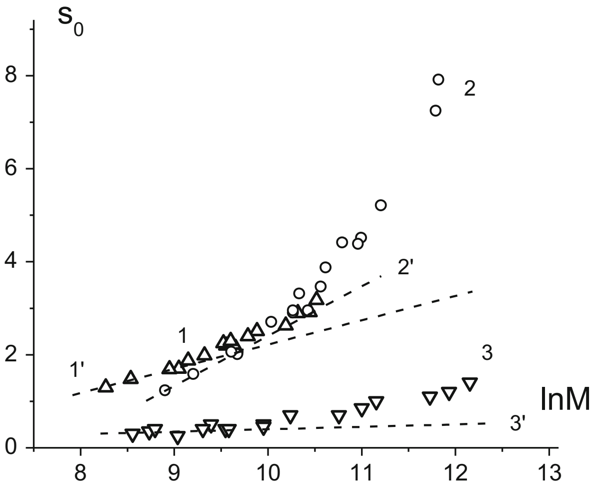

Fig. 14.8 Determination of mass per unit length M_L, the ratio of mass M to contour length L, and the hydrodynamic diameter d of heparin in 0.2 M NaCl (1and 1′) (Pavlov et al. 2003), poly{4-[4-(hexyloxy)phenyl]ethynylphenyl methacrylate} in toluene (2 and 2′) (Pavlov et al. 2012), and poly(2,2′-p-phenylene-(5-benzimidazole)) isophthalamide in dimethylacetamide + 3 % LiCl (3 and 3′) (Pavlov et al. 1985) from the plot of s_0 versus ln M. The linear extrapolation (dashed line 1′, 2′, and 3′) was made using the fractions of smallest M. The slope and intercept allow to determine M_L and d, respectively, within the framework of the weakly bending rod model or the cylinder model (Eq. 14.23), usable in the theoretical limit of $L/A < 2.3$. For heparin chain, the following results were obtained: $M_L = (570 \pm 50)$ g × mol^{-1}nm^{-1} and $d = (0.9 \pm 0.1)$ nm, for poly{4-[4-(hexyloxy)phenyl]ethynylphenyl methacrylate} chain M_L was equal to (1520 ± 60) and d was equal to (2.1 ± 0.1). The data obtained for polyamide benzimidazole macromolecules did not contradict to the theoretical value of $M_L = 190$

molecules. The long-range effects are apparent in very long chains regardless of their stiffness, but it is easier to observe and study the long-range interactions in the flexible polymers. In the case of flexible polymers, the chain is contracted significantly, and there is a high probability of interaction between the remote chain monomer units. The most part of polymer coil becomes impermeable for a solvent; flexible macromolecules manifest the effects of thermodynamic interaction between polymeric material and solvent molecules.

The detailed modeling theories of hydrodynamic characteristics are elaborated for two models of macromolecules *without the volume effects*: wormlike necklace (Hearst and Stokmayer 1962; Hearst 1964) and wormlike cylinder (Yamakawa and Fujii 1973, 1974). These model theories do not take into account the excluded volume effects and attribute the change in coil size solely to the change in persistence length. Note that in the case of chains without volume interactions, the b_η index varies from 1.8 for slightly bending rod (very stiff and/or very short chains) to 0.5 for a Gaussian coil (very long chain independently of the rigidity). Meanwhile, in the case of the chain with volume interactions, the b_η index varies from 0.8 for long chains with strong volume interactions to 0.5 for a Gaussian coil (no volume interactions or very short flexible chains). The procedure taking into account the influence of volume effects on transport characteristics was developed on the basis of linear approximation of the dependence of swelling coefficient of flexible macromolecules (α) on the excluded volume parameter (z),

$$\alpha = \left[< h^2 > / < h^2 >_\theta \right]^{1/2} = 1 + Cz + \cdots , \qquad (14.25)$$

where $< h^2 >$, $< h^2 >_\theta$ are the size of the swelling coil and the size of the coil in θ-conditions, respectively. The numerical coefficient C for short chains depends on the relative contour length (L/A), $C = C(L/A)$, and with increasing chain length, the C value tends to the limit $C = 4/3$ (Yamakawa and Stockmayer 1972). The excluded volume parameter z describes the number of collisions between chain segments per unit volume occupied by the macromolecule. Finally for flexible chains with moderate excluded volume effects, the data on translation friction are treated with the aid of the Cowie-Bywater plot (1965), and the data on intrinsic viscosity are processed using the Burchard-Stockmayer-Fixman plot (1961; 1963). In this case, the change of the coil size is related exclusively to the change in the thermodynamic quality of the solvent.

Up to now, the more complete theory that takes into account the simultaneous influence of draining and excluded volume effects on the translation friction coefficient is Gray-Bloomfield-Hearst (GBH) theory (1967). Unfortunately, this translation friction (sedimentation) coefficient theory has found insufficient dissemination and application, apparently, because the corresponding equation has not been represented in an easy form to use. In the case of the intrinsic viscosity theory (Sharp and Bloomfield 1968), the authors have received only an asymptotic expression for extremely large values of molar mass.

The sedimentation coefficient calculations (Gray et al. 1967) were carried out for distant segment pairs using the parameter ε which characterizes the deviations of the mean-square end-to-end distance from the Gaussian form due to volume swelling effects ($< h^2 > \sim M^{1+\varepsilon}$). For close segment pairs, when volume interactions are small, the Porod-Kratky statistics have been applied. The analytical result for the velocity sedimentation coefficient is given in Eq. (14.10) in Gray et al. (1967, p.1495). This equation may be rearranged for $L/A > 2.3$ in a more compact form as shown in Pavlov et al. (1990):

$$\begin{aligned}[s]P_0 N_A = {} & (3/(1-\varepsilon)(3-\varepsilon)(M_L{}^{(1+\varepsilon)/2}/A^{(1-\varepsilon)/2})M^{(1-\varepsilon)/2} \\ & + (M_L P_0/3\pi)\left[ln\,(A/d) - (d/3A) - \varphi(\varepsilon)\right] \end{aligned} \qquad (14.26)$$

where P_0 and Φ_0 are Flory hydrodynamic coefficients and $\varphi(\varepsilon) = 1.431 + 2.635\varepsilon + 4.709\varepsilon^2 + \cdots$.

In the case of $\varepsilon = 0$, i.e., in the absence of the intrachain excluded volume effects, Eq. 14.26 is transformed into the expressions obtained in the theories of Hearst and Stockmayer (1962) and Yamakawa and Fujii (1973):

$$[s]\,N_A P_0 = (M_L/A)^{1/2} M^{1/2} + (P_0 M_L/3\pi)\left[ln(A/d\,(A/d)\ -\varphi(0)\right] \tag{14.27}$$

where φ(0) depends on the model used (φ(0) = 1.431 for the wormlike necklace model (Hearst and Stokmayer 1962) or φ(0) = 1.056 for the wormlike cylinder model (Yamakawa and Fujii 1973), respectively).

Viscometry data in the range of the molar mass values when $L/A > 2.3$ may be treated by changing the variables $[s]P_0N_A = (M^2\Phi_0/[\eta])^{1/3}$ according to Pavlov et al. (1990) and using the corresponding relationship (Eq. 14.26). When $L/A > 2.3$, linear approximations of the s_0 and/or $(M^2/[\eta])^{1/3}$ vs. $M^{(1-\varepsilon)/2}$ may be applied (Eqs. 14.26 and 14.27). The slope of these straight lines allows evaluation of the chain persistence length, and the intercept allows estimating the hydrodynamic diameter of the chain. Some examples are presented in Fig. 14.9, i.e., the treatments of data using the s_0 and $[\eta]$ values for two different systems (polyamide benzimidazole in DMAA + 3 % LiCl at 21° C (Pavlov et al. 1985) and polyisobutylene in n-heptane at 25° C (Abe et al. 1993)).

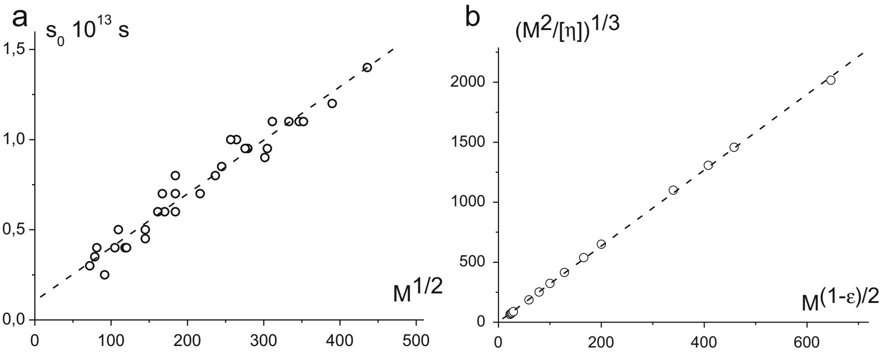

Fig. 14.9 Dependences of s_0 (**a**) and $(M^2/[\eta])^{1/3}$ (**b**) on $M^{(1-\varepsilon)/2}$ used for the estimation of the statistical segment length A (or the persistent length $a = A/2$) and the hydrodynamic diameter d in correspondence with the Gray-Bloomfield-Hearst theory (relationships (25)) for polyamide benzimidazole fractions in DMAA + 3 % LiCl at 21 °C (**a**) and polyisobutylene in n-heptane at 25 °C (**b**) of different sizes. For polyamide benzimidazole macromolecules (Pavlov et al. 1985), the following estimations were obtained: the parameter $\varepsilon = 0$, the values $A_f = (6.9 \pm 0.7)$ nm, and $d_f = (0.4 \pm 0.2)$ nm with $P_0 = 6.0$ (Fig. 14.9a). For polyisobutylene macromolecules (Abe et al. 1993), correspondingly, $\varepsilon = 0.10$, $A_\eta = (1.40 \pm 0.01)$ nm, and $d_\eta = (0.20 \pm 0.07)$ nm with $\Phi_0 = 2.3 \times 10^{23}$ (Fig. 14.9b)

14.10 Multi-Hydfit Program

In the relatively recent works of de la Torre and his colleagues (Ortega and de la Torre 2007, 2013; Amoros et al. 2011), a method of computer processing of the experimental data obtained in independent experiments is developed. The aim of this approach is to obtain the structural and conformational parameters of linear macromolecules. The authors introduce the dimensionless ratio of the experimental values to the corresponding values for the rigid sphere (concept of bead-model hydrodynamics (de la Torre and Bloomfield 1981)). The persistence length, diameter, and mass per unit length can be evaluated using Multi-Hydfit program; this program performs a minimization procedure aimed at finding the best values of a, d, and M_L, satisfying the equations which describe hydrodynamic behavior of persistence cylinders without the excluded volume effects (Yamakawa and Fujii 1973, 1974). The Multi-Hydfit program then "floats" the variable parameters in order to find a minimum of the multi-sample error function (Ortega and Torre 2007), which is calculated using equivalent radii. The equivalent radius is defined as a radius of an equivalent sphere having the same value as the determined characteristic (translation diffusion and/or velocity sedimentation coefficients and intrinsic viscosity). The error function is a dimensionless estimate of the agreement between the experimentally measured characteristic and the theoretical values of a, d, and M_L calculated for the selected hydrodynamic characteristic and for a particular molar mass. The last version of program also includes the option for chains with the excluded volume effects, e.g., for poly(isobutylene) in n-heptane (Amoros et al. 2011). This important addition concerns on a huge class of flexible chain polymers, both synthetic and natural origin.

The final results of Multi-Hydfit program are presented as the maps of conformation-structural parameters like the topographic maps. This is illustrated in Fig. 14.10 which demonstrates the result of handling hydrodynamic data by Hydfit program. The measurements were performed on a series of samples of alternating styrene/diphenylethylene copolymers functionalized with terpyridine in toluene solutions; the molecular mass range was $1.7 < M \times 10^{-3}$ g/mol <25.2 (Pavlov et al. 2009).

14.11 Further Steps of the Analysis of the Hydrodynamics Data of Homologous Series of Linear Macromolecules

It should be noted that as well as for non-computerized procedures, the sought-for estimates are more adequate, the wider is the range of studied molecular masses. It is especially important to have a sufficient number of samples of low molecular masses, when L/A is less than 2, to obtain the reliable and adequate value of M_L. However, the choice between intramolecular effects of excluded volume and/or of intrachain draining in doubtful cases of semiflexible macromolecules is beyond the

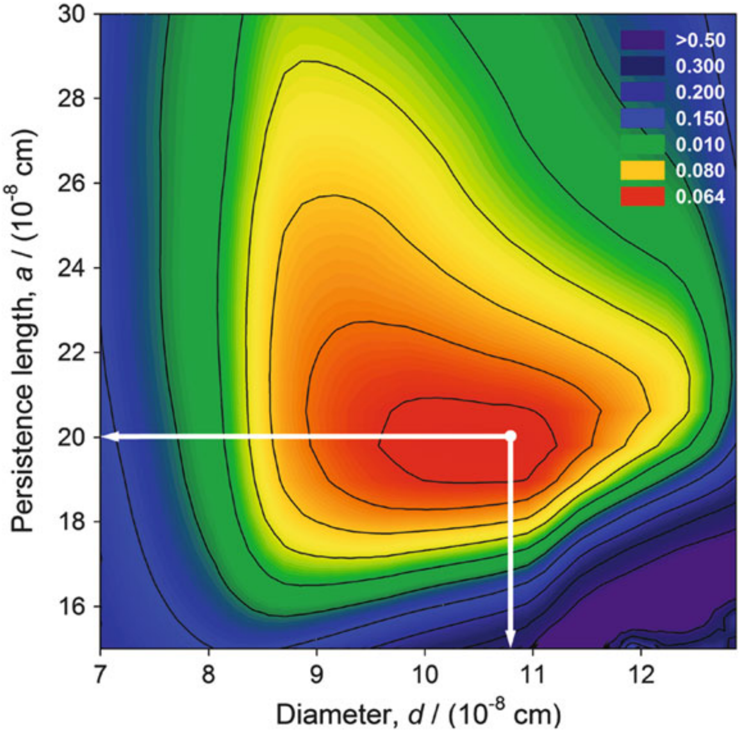

Fig. 14.10 Hydfit contour plot of the percent typical deviation, 100Δ, of the alternating styrene/diphenylethylene copolymers functionalized with terpyridine molecule in toluene with a fixed value of $M_L = 564$ g/(mol nm), showing the minimum of the deviation at the following values of persistence length, $a = 2$ nm and $d = 1.1$ nm (Pavlov et al. 2009)

capabilities of these approaches. One unresolved macromolecular hydrodynamic problem concerns the partition of the influence of the draining and volume effects on the size of the macromolecular chain. The value of parameter ε can/should be divided into two components: one is responsible for the volume effects (ε_v) and the other one for the flow of solvent molecules through the polymer coil (ε_d): $\varepsilon = \varepsilon_v + \varepsilon_d$. In Eq. 14.26, only the ε_v part should be used for estimating statistical segment length and hydrodynamic diameter.

Finally, generalization of the hydrodynamic data, namely, the intrinsic viscosity and velocity sedimentation coefficient values can be made by the double normalization of the canonical KMHS equations by the structural parameter M_L and the statistical segment length A taking into account the both parameters (Pavlov et al. 1999; Pavlov 2005, 2007). In this procedure, the chain contour length L is calculated for a unit of the statistical segment length A, i.e., (L/A). The fundamental

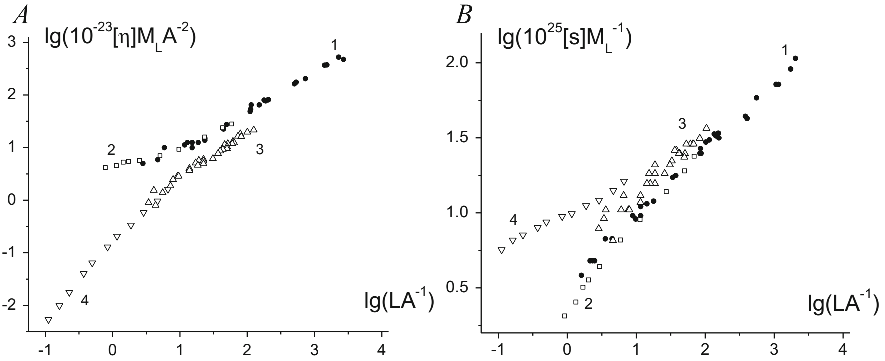

Fig. 14.11 Double normalized plots of $[\eta]M_LA^2$ (**a**) and $[s]M_L{}^{-1}$(**b**) vs. relative contour length LA^{-1} presented in double logarithmic scale. This figure interprets the data given in Fig. 14.5. Comparison of linear macromolecules of different structures, different equilibrium rigidities, and different scaling indices was made; these macromolecules are poly(1-vinyl-2-pyrrolidone) in 0.1 M sodium acetate solutions (*1*), styrene-methyl methacrylate brush copolymer in bromoform (*2*), poly(2,2′-p-phenylene-(5-benzimidazole)) isophthalamide in dimethylacetamide +3 % LiCl (*3*), and the triple helix of *Schizophyllum commune* polysaccharide (schizophyllan) in water (*4*). The following lengths of the statistical segment $A \times 10^8$ cm and the relative hydrodynamic diameters (*d*/*A*) are obtained for comparing macromolecules: 22 and 0.2 (1), 90 and 0.5 (2), 90 and 0.06 (3), 4000 and 0.007 (4)

Flory-Fox (14.4) and Svedberg (14.6) equations can be transformed into the following relationships:

$$[\eta]\,M_L/A^2 = \Phi\,(L/A,\ d/A, \varepsilon) \times (L/A)^{1/2} \tag{14.28}$$

$$[s]\,/M_L = (P\ \ (L/A,\ d/A, \varepsilon)\,N_A)^{-1} \times (L/A)^{1/2} \tag{14.29}$$

where *L/A* is the relative contour length and *d/A* is the relative chain diameter.

Figure 14.11 shows the data plotted in Fig. 14.5 in new coordinates $[\eta]$ M_L/A^2 and *[s]/*M_L *vs.* relative contour length *L/A*. These plots (Fig. 14.11) illustrate the earlier conclusion (Pavlov 2013; Pavlov et al. 2014) that the entire set of the linear macromolecules, regardless of the stiffness realization mechanism (free/hindered rotation around valence bonds, multistrand helix structures, electrostatic and/or thermodynamic interactions, specific interactions that lead to the globule formation), obeys the same laws.

14.12 Examples of Handling of Velocity Sedimentation Data with Sedfit Suite

To estimate the value of sedimentation coefficient for a series of fractions/samples of polymers from the files of raw data obtained with the XLI analytical ultracentrifuge (usually, using the interference optics), the Sedfit suite software may be chosen. This program provides the opportunity to process the velocity sedimentation data (Schuck 2000; Dam and Schuck 2004; Schuck and Zhao 2011). Within the framework of this suite, the raw data can be processed using various programs, and the results can be compared to each other. The treatment of the results obtained in the sedimentation experiments with different linear polymers in the wide range of molar masses will be discussed below.

14.12.1 Model-Less Method for Calculating the Apparent Differential Sedimentation Coefficient Distribution g(s)*

First, the model-less method for calculating the apparent differential sedimentation coefficient distribution $g^*(s)$ denoted by ls$-g^*(s)$ (Schuck and Rossmanith 2000) is employed; this method involves direct linear least-squares boundary modeling with the aid of superposition of sedimentation profiles of ideal *nondiffusing particles* (Figs. 14.12 and 14.13). This model is appropriate for the high molar mass polymer when the diffusion flow is slow and the s/D ratio is more than ≈ 0.3 svedberg/fick (1 svedberg $= 10^{-13}$ s and 1 fick $= 10^{-7}$ cm^2/s). Despite the fact that the average sedimentation coefficient does not differ from the values obtained using other models, the obtained distribution ls-$g^*(s)$ does not reflect the real distribution of sedimentation coefficients (molar masses) because it contains unaccounted diffusion spreading.

In some cases, the additional *ls−g*(s) model with one discrete Lamm equation component* completes the distribution curve in the region of small s values and, respectively, in the range of large D values (Fig. 14.13). This variation of the model not only serves an aesthetic purpose but also is entirely consistent with the general idea that linear synthetic and natural polymers have the essentially continuous molar mass distributions.

The results obtained using different up-to-date software should be compared to those obtained by the classical method based on the definition of sedimentation coefficient: $s \equiv (d\ln r/dt)\omega^{-2}$, where r is the position of sedimentation boundary, ω is the angular velocity, and t is the time of sedimentation (Svedberg and Pedersen 1940). The integral curves can be transformed into differential ones. Two kinds of differentiation are possible. First, the value of dJ/dr is calculated by differentiation of the raw interference curve with the subsequent smoothing. The second way is to compute dJ/dt curves as the difference of the adjacent interference curves when the

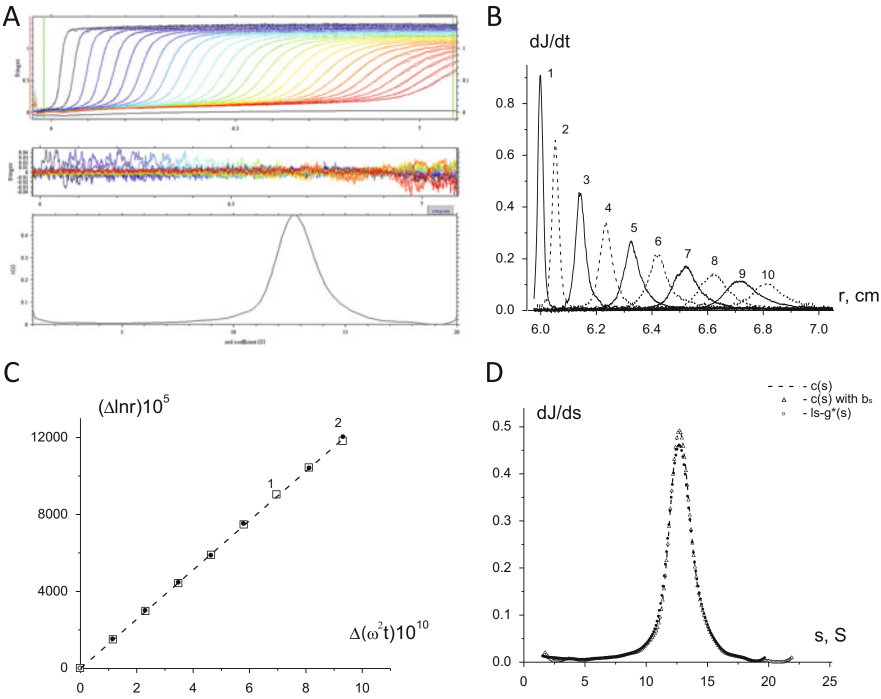

Fig. 14.12 Results obtained in the velocity sedimentation experiments using a pullulan standard (Polymer Standards Service GmbH) with $M_w = 1\ 660$ kg mol^{-1} and a concentration $c = 0.54$ mg cm^{-3} in H_2O at 25 °C, at a rotor speed of 42,000 rpm (Pavlov and Ebel 2006). (**a**) *Top*, superposition of the integral distribution of the pullulan concentration inside the cell collected by interference optics every 240 s; *middle*, corresponding residuals plot obtained by the Sedfit – $c(s)$; *bottom*, distribution obtained with $c(s)$ model. (**b**) Corresponding differential distribution of the sedimentation profiles *dJ/dt*. (**c**) Dependence of Δlnx on Δt; the slope of this dependence yields $s \equiv d\ln r/d(t\omega^{-2}) = 12.8$ S, $1 - dJ/dt$, $2 - dJ/dr$. (**d**) Comparison of the differential distributions of the sedimentation coefficient obtained by different model of Sedfit suite: (1) $c(s)$, $s = 12.78$ S; (2) $ls - g^*(s)$, $s = 12.79$ S; and (3) $c(s)$—bs, $s = 12.64$ S. Thus, the average of the four values is $s = (12.75 \pm 0.04)$ S, and the maximum difference between the obtained values $\Delta s = 0.16$S amounts 1.2 % from the mean value (insignificant deviation)

shift in time is small (Stafford 1994) (Fig. 14.12b, c). The slope of the dependence of the sedimentation boundary shift logarithm ln$r$ on $\omega^2 t$ allows to evaluate the sedimentation coefficient by its definition.

It is necessary to point out that the study of the concentration dependence of the velocity sedimentation is an important task in the hydrodynamic investigation of linear polymers (Eq.14.11 and Fig. 14.14).

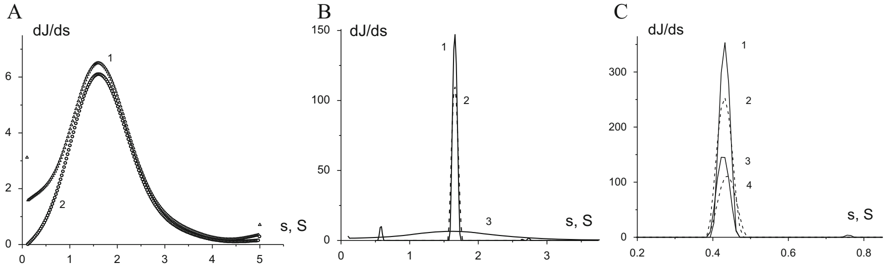

Fig. 14.13 Comparison of differential distributions obtained with different model of Sedfit suite. (**a**) Differential distributions *dJ/ds* of a pullulan sample with $M_w = 11.8$ kg/mol in H_2O at $c = 5.38$ mg/cm^3 obtained with $ls{-}g^*(s)$ model (1) and with $ls{-}g^*(s)$ with one discrete Lamm Eq. component model (14.2). The last model gives more realistic dependence in the region of very low s values. (**b**) The distributions of sedimentation coefficients obtained for the same sample. The following values were obtained with the different model of Sedfit program: continuous $c(s)$ distribution – $s = 1.65$ S (2); continuous $c(s){-}bs$, $b_s = 0.458$ – $s = 1.66$ S (1); and $ls - g^*(s)$ – $s = 1.7$ S (3). In the case of the low molar mass sample which is characterized by the high diffusion coefficient ($D_0 \approx 10 \times 10^{-7}$ cm^2/s), there is a striking difference in the form of $ls{-}g^*(s)$ distributions. Here, the diffusion process is not taken into account, which leads to a fictitious broad distribution as compared with two other methods ($c(s)$ and $c(s){-}bs$). These two methods take into account the dominant diffusion flux during sedimentation. At the same time, the average sedimentation coefficient obtained by $ls{-}g^*(s)$ method virtually is the same as those obtained with two other methods. For this sample, the ratio s_0/D_0 is ≈ 0.17 svedberg/fick. (**c**) Distributions of sedimentation coefficients obtained for the fraction of poly(N-methyl-N-vinylacetamide) with $M_{sD} = 5.2$ kg/mol in H_2O at $n = 40{,}000$ rpm. The following values were obtained using the different models included in Sedfit program at the concentration $c = 3.03$ mg/cm^3 (1 and 2): continuous $c(s)$ distribution – $s = 0.43$S (1); continuous $c(s){-}bs$, $b_s = 0.43 - s = 0.43$S (2); at the concentration $c = 1.5$ mg/cm^3 (3 and 4), continuous $c(s)$ distribution – $s = 0.44$S (3); continuous $c(s){-}bs$, $b_s = 0.43$ – $s = 0.43$S (4). It is noteworthy that, in the case when the sedimentation flow becomes wilted, and the diffusion flow is growing ($D_0 \approx 13 \times 10^{-7}$ cm^2/s), the $ls{-}g^*(s)$ model is no longer applicable for evaluating the velocity sedimentation coefficient. For this sample, the ratio s_0/D_0 is ≈ 0.03 svedberg/fick (Pavlov et al. 2010a)

14.12.2 Continuous c(s) Model in Sedfit Suite

Second, the differential distribution of sedimentation coefficient $c(s)$ is calculated by numerical solution of Lamm equation in which both opposite flows (sedimentation and diffusion) are taken into account (*continuous c(s) model*, Schuck 2000). In order to achieve one-parametric distribution, a scaling law between the diffusion and sedimentation coefficient is invoked in the $c(s)$ method. The choice of the scaling law is based on the $D_0 = K_{Ds}s_0{}^{-1/2}$ relation which is correct for roughly globular particles, with the frictional ratio (f/f_{sph}) as a scaling parameter (f is the frictional coefficient of the solute macromolecule; f_{sph} is the frictional coefficient of a rigid sphere with the same "anhydrous" volume (free of solvent) as the macromolecule). Fitting for (f/f_{sph}) in a nonlinear regression will provide the estimate of the weight-average frictional ratio of all macromolecules in solution that actually leads to

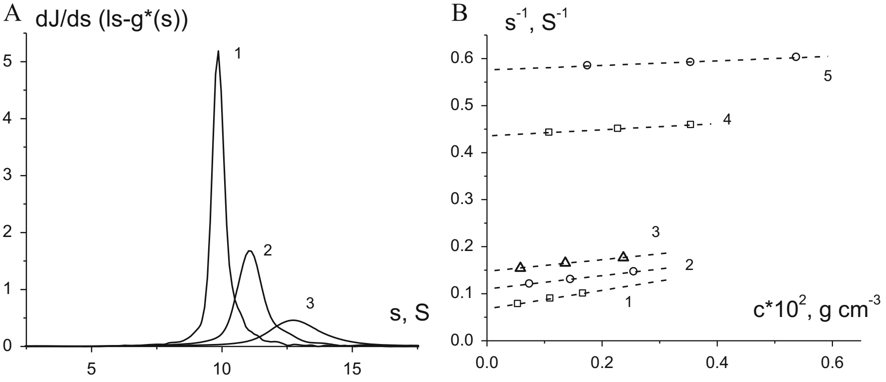

Fig. 14.14 Concentration dependence of velocity sedimentation for pullulan molecules in H_2O, $n = 42{,}000$ rpm, at 25°C. (**a**) Distributions obtained using $ls - g^*(s)$ model for sample with $M_w = 1660$ kg/mol at different concentrations: (1) $c = 1.67$, (2) $c = 1.10$, and (3) $c = 0.54$ mg/cm^3. The area under the distribution curve gives the number of fringes J and corresponds to polymer concentration c. The refractive index increment was calculated from $(\Delta n/\Delta c) = \mathrm{J}\lambda/Kcl$, where λ is the wavelength, K is the magnifying coefficient, and l is the optical path length. (**b**) Concentration dependences of the (reciprocal) sedimentation coefficient s^{-1} for pullulan samples of different molar masses and corresponding characteristics s_0 and k_s: (1) $M_w = 1\ 660$ kg/mol, $s_0 = 14.8$ S, $k_s = 290$ cm^3/g; (2) $M_w = 404$, $s_0 = 9.1$, $k_s = 130$; (3) $M_w = 212$, $s_0 = 6.8$, $k_s = 80$; (4) $M_w = 22.8$, $s_0 = 2.3$, $k_s = 15$; and (5) $M_w = 11.8$, $s_0 = 1.7$, $k_s = 8$

determination of the average value of the translational diffusion coefficient D:

$$D_0 = kT(1 - \upsilon\rho_0)^{1/2}/\eta_0{}^{3/2}\left(9\pi 2^{1/2}\right)\left(f/f_{sph}\right)_0{}^{3/2}(s_0\upsilon)^{1/2} \tag{14.30}$$

The distribution of the sedimentation coefficients for the sample in Sedfit software is denoted as c (s). Usually this kind of designation is used for integral distribution. Indeed, c is a concentration; in the case of interference optics, it is expressed as a number of fringes J, which is unambiguously associated with the concentration; see the relation (14.31). However, the Sedfit program gives the distribution in a differential form. The area under the differential curve is equal to the number of interference fringes (i.e., concentration). Therefore, it is logical and more consistent to denote this distribution by $dc(s)/ds$ or $dJ(s)/ds$. Finally, the differential distribution ($dc(s)/ds$) of the sample is obtained (Figs. 14.12 and 14.13). The area under the $dc(s)/ds$ curve gives the loading concentration of the macromolecules between the minimum and maximum s-value occurring (expressed in number of fringes, J). Note that the concentration dependence of J (fringes number) allows defining an additional parameter – the refractive index increment $\Delta n/\Delta c$

$$\Delta n/\Delta c = J\lambda/Kcl \tag{14.31}$$

where λ is the wavelength, K is the magnifying coefficient, and l is the optical path length. The value of $\Delta n/\Delta c$ is a characteristic of polymer-solvent system and should be virtually constant in a series of polymer homologues until the oligomer region. Obviously, such correlation will be performed in the case of an absorption boundary registration: $OD_{solution} = OD_{solvent} + K_{ab}c$, where K_{ab} is the increment of the polymer absorption in a given solvent ($K_{ab} \equiv dOD/dc$). However, this relationship will hold within the range of much smaller concentration due to quick absorbance saturation.

Needless to say, the series of globular particles is not the best model to describe hydrodynamic behavior of linear macromolecules. Nevertheless, the continuous $c(s)$ distribution model leads to reasonable values of the velocity sedimentation coefficients for many linear polymers.

14.12.3 Continuous c(s) Model with General Scaling Law in Sedfit Suite

Third, recently Sedfit suite has been implemented with *continuous c(s) model with general scaling law* (designated below as $c(s)$–bs). Some information about this add-in program is contained in a publication by Harding et al. (2011b). In this paper, the implementation is called "extended Fujita approach." For direct boundary modeling with distributions of the Lamm equation solutions (Schuck 2000), the measured interference (or absorbance) profiles $a(r, t)$ were modeled as an integral over the differential concentration distribution $c(s)$

$$a\,(r,\ t) = \int c(s)\chi\,(s,\ D(s),\ r,\ t)\ ds + b_{nr}(r) + b_{nt}(t) \tag{14.32}$$

with b_{nr} (r) and $b_{nt}(t)$, denoting systematic baseline noise components, and $\chi(s, D(s), r, t)$ denoting the solution of the Lamm equation at unit loading concentration of a species with sedimentation coefficient s and diffusion coefficient D

$$d\chi/dt = r^{-1}d\left[rD(s)\,(d\chi/dr) - s\omega^2r^2\chi\right]/dr \tag{14.33}$$

where r is the distance from the center of rotation and ω is the rotor angular velocity. Equation 14.33 was solved by finite element methods in a static or moving frame of reference as described in Claverie et al. (1975), Schuck (1998), and Schuck (1998). For each species, the diffusion coefficient $D(s)$ was estimated as a function of the sedimentation coefficient s based on the general scaling law, which may be presented as

$$D_0 = \Big(RT/\,(1 - \upsilon\rho_0)\,{K_s}^{1/bs}{s_0}^{(bs-1)/bs} = K_{Ds} \times s^{(bs-1)/bs} \tag{14.34}$$

where the parameters b_s and K_s define the scaling relation between s_0 and M ($s_0 = K_s M^{bs}$). It should be emphasized that the $D_0 = K_{Ds} s_0{}^{-1/2}$ relation known for globular species is a special case of general Eq. 14.34. To solve the Lamm equation numerically, the range of possible velocity sedimentation coefficient values is typically discretized into 100–200 values. Actually, it is modern paraphrase of the "graphic fractionation" approach (Gralen 1944; Kinell and Ranby 1950). For any reasons, a researcher specifies the power law exponent b_s, and the program fits the best value of $K_s{}^*$. The asterisk means that this value is obtained at some known concentration, and these values must be extrapolated to zero concentration to obtain the non-disturbed K_s value. In the finite element method, the solutions of the ideal Lamm equation are obtained using the adaptive grid algorithm which allows fitting the best $K_s{}^*$ value; finally, each s-value gets the corresponding D-value. As a result, the differential distribution ($dc(s)/ds$) of the sample is also fitted. The relation (14.34) has a general meaning and may be applied to any kind of homologous series of the macromolecular compounds. In principle, the $c(s){-}bs$ implementation is more appropriate to treat the velocity sedimentation data on any macromolecules due to the possibly large variation of the b_s value. The K_s value (Eq. 14.15) should not be confused with the Gralen concentration coefficient k_s (Eqs. 14.7).

Note that the distributions of the sedimentation coefficients for the samples of high molar masses obtained using different models ($c(s)$, $c(s){-}bs$, and $ls - g^*(s)$) are virtually indistinguishable (Fig. 14.12d). The lower the molar mass, the higher the deviation of the $ls - g^*(s)$ distribution from the real one (Fig. 14.13b). However, up to a certain value of the s/D ratio (>0.2), the average value of sedimentation coefficient s obtained using the $ls - g^*(s)$ model is almost equal to the average values of s obtained with the use of other models.

Another important question arises: How do the fitted $K_s{}^*$ values sort with those obtained by the straightforward procedure of comparison between the s_0 values and molar masses for a series of samples? The results obtained for the flexible polymers are summarized in Figs. 14.15, 14.16, and 14.17, and the following conclusions can be draw from these data. Uppermost, the $K_s{}^*$ value strongly depends on concentration. This fact highlights the importance of studying the concentration dependencies of the hydrodynamic characteristics in the appropriate range of concentrations and extrapolating the sought-for characteristics to infinite dilution. This means that the use of a single concentration for estimating samples polydispersity is unlikely to give the reliable results.

The sign of the slope of concentration dependence is determined by the thermodynamic quality of the solvent (compare Figs. 14.15 and 14.17 with Fig. 14.16). The $K_s{}^*$ values depend in a unified manner on the parameters characterizing the degree of dilution ($c[\eta]$ or ck_s) of samples of different molar masses. The fitted K_s values extrapolated to the infinite dilution are close to those obtained in the traditional way. Here is another proof of self-sufficiency of the velocity sedimentation method coupled with the Sedfit $c(s){-}bs$ model in the determination of molecular characteristics of linear polymers.

Explicitly, the use of new software for primary processing of the experimental data should lead to results, which must not contradict with the main conclusions on

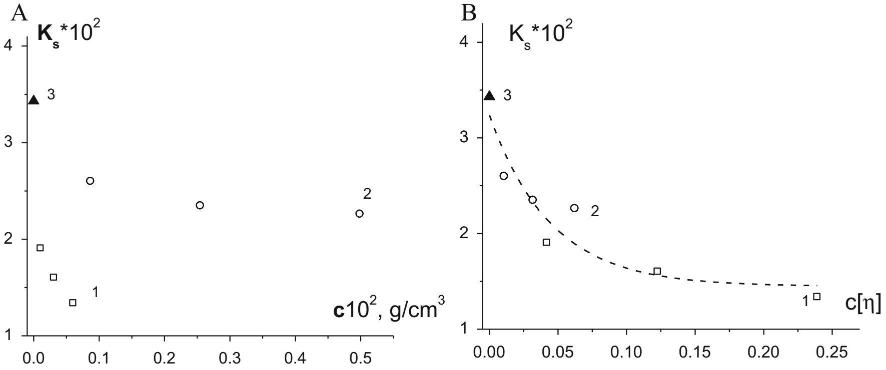

Fig. 14.15 Concentration dependences of fitted K_s^* value parameter (**a**) for polystyrenes of different molar masses in toluene (which is thermodynamically good solvent for polystyrene): (1) $M = 1760$, (2) $M = 17$ kg/mol; dependences of K_s on the $c[\eta]$ parameter (**b**). Triangle point (3) is the K_s value from the independent literature data (Meyerhoff and Appelt 1979). K_s^* values are fitted within the framework of the continuous $c(s)$ model with general scaling law $D_0 = RT/(1 - \upsilon\rho_0)K_s{}^{1/bs}s_0{}^{(bs-1)/bs} = K_{Ds} \times s^{(bs-1)/bs}$. K_s^* is not to be confused with the concentration Gralen coefficient k_s in Eq. 14.11

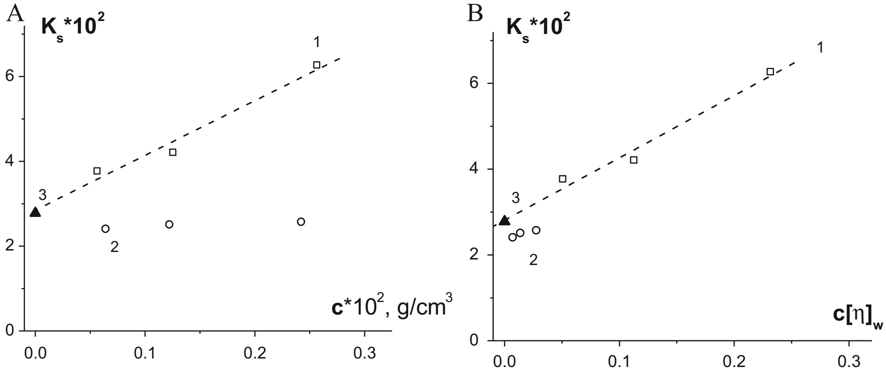

Fig. 14.16 Concentration dependences of fitted K_s^* value (**a**) for two mixtures of polystyrene standards of different molar masses studied in MEK (which is a marginal solvent for polystyrene) and dependences of K_s^* on the dilution parameter $c[\eta]$ (**b**). Full triangle point is the K_s value from the independent literature data (Pavlov et al. 2011). (1) $(1760 + 1060 + 710 + 311 + 194) \times 10^3$ g/mol, 20 % of each in the mixture, $[\eta]_w = \Sigma(0.2[\eta]_i) = 90.2$ cm^3/g; (2) $(95 + 43 + 9 + 4 + 1.8) \times 10^3$ g/mol, 20 % of each in the mixture, $[\eta]_w = \Sigma(0.2[\eta]_i) = 11.6$ cm^3/g, where $[\eta]_i$ is the intrinsic viscosity value of the individual sample

conformational states of linear macromolecules that have been previously received on the basis of the velocity sedimentation coefficients obtained with the fundamental relations. This is true, at least for the flexible linear polymers.

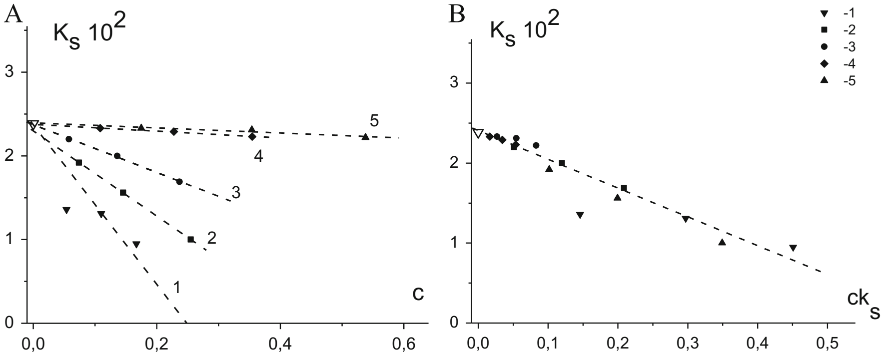

Fig. 14.17 Concentration dependences of fitted K_s^* value (**a**) for pullulan of different molar masses (kg/mol) in H_2O (which is thermodynamically good solvent for pullulan): (1) $M = 1660 \times 10^3$ g/mol, (2) $M = 404$, (3) 212, (4) 22.8, (5) 11.8×10^3 g/mol (*left side*) and K_s^* dependences on the ck_s parameter characterizing the degree of solution dilution (**b**). Open triangle point is the K_s value from the literature data (Pavlov et al. 1994 and the references therein). K_s^* is not to be confused with the concentration Gralen coefficient k_s in Eq. 14.11

14.13 Conclusions

Self-sufficiency of the velocity sedimentation method manifests itself (1) in the qualitative analysis of the conformational status of linear macromolecule from the lgk_sM_L vs. $lg\ [s]/M_L$ plot, (2) in the possibility of an adequate assessment of polymer molar masses and further conformational analysis using the sedimentation parameter β_s, and (3) in the fact that numerical solution of the Lamm equation using the $c(s)$–bs model within Sedfit suite allows to set the scaling relation $s_0 = K_sM^{bs}$ which opens up possibilities for further conformational analysis, as well as molar mass distribution analysis.

In outcome conclusion, we propose the following algorithm for the study of homologous series of macromolecules using XLI coupled with $c(s)$–bs model inside of Sedfit suite.

The proposed algorithm involves the following stages:

0. First of all, for the comprehensive and exhaustive study of any polymer system, the researcher should have a set of samples/fractions with narrow polydispersity and the possibly broadest range of molar masses.
1. Studying of the concentration dependence of the available number of samples/fractions using $c(s)$ or/and $ls - g^*(s)$ models of Sedfit suite.
2. Determining the s_0 and k_s values from the concentration dependencies of s^{-1} and subsequently establishing the $k_s = K_{sks}{s_0}^{bks}$ correlation in order to define the scaling index b_s in the KMHS-type relation $s_0 = K_sM^{bs}$ from the $b_{ks} = (2 - 3b_s)/b_s$ relationship.
3. Using the obtained b_s value, the rehandling of raw set of data must be done using $c(s)$–bs model and $K_s{*}(c)$ parameter must be fitted. The concentration

dependencies of K_s* must be plotted and extrapolated to zero concentration conditions. Thus, the unperturbed value of K_s will be estimated and the scaling relation $s_0 = K_s M^{bs}$ is known.

4. The molar masses M may be calculated. It is necessary to check the b_s and K_s values using the double logarithmic plot (lgs_0 vs. lgM). The difference of about $\Delta b_s \approx 0.01$ can be considered as insignificant. But if, for example, instead of $b_s = 0.41$, the b_s value turns out to be $b_s = 0.46$, it is necessary to go back to step 3 and repeat the process using the new value $b_s = 0.46$. In other words, the method of successive approximations is necessary to achieve the consistency in the b_s value.
5. With the final set of s_0, k_s, and M values, further molecular interpretation may be reached: assessments of the sedimentation parameter β_s values, Kuhn segment length, the value of hydrodynamic diameter, the degree of macromolecular coiling, etc. Finally, the obtained estimations should be compared with the chemical structure of the repeating unit of the polymer.
6. If successful, this path gives the full set of molecular and conformation characteristics of studied linear polymer and will illustrate self-sufficiency of the sedimentation velocity method in the study of a homologous series of linear polymers.

Finally, it is interesting to analyze possible scope of measuring sedimentation coefficients with the help of the modern analytical ultracentrifuge. The upper limit can be represented by sedimentation of nanoparticles and nano-complexes, and it totals hundreds of thousands of svedberg (e.g., Perevyazko et al. 2010, 2012). Up to now, the lower limit has been apparently achieved in the studies of the cyclodextrins, and it is about one tenth of svedberg (Pavlov et al. 2010b). Thus, one XLI instrument enables us to measure the values of a physical quantity differing by six orders of magnitude (by varying the rotation speed and/or solvent). This is a rare opportunity in the practice of physical experiments.

Acknowledgments GMP is grateful to Dr. O.V. Okatova for her help in preparing this manuscript. This work was partially supported by the St. Petersburg State University research grant (11.38.267.2014).

References

Abe F, Einaga Y, Yamakawa H (1993) Excluded-volume effects on the intrinsic viscosity of oligomers and polymers of styrene and isobutylene. Macromolecules 26:1891

Amoros D, Ortega A, de la Torre GJ (2011) Hydrodynamic properties of wormlike macromolecules: monte carlo simulation and global analysis of experimental data. Macromolecules 44:5788

Behlke J, Ristau O (1997) Molecular mass determination by sedimentation velocity experiments and direct fitting of the concentration profiles. Biophys J 72:428

Benoit H, Doty PM (1953) Light scattering from non-Gaussian chains. J Phys Chem 57:958

Bernal JMG, Tirado MM, Freire JJ, de la Torre JG (1991) Monte Carlo calculation of hydrodynamic properties of linear and cyclic polymers in good solvents. Macromolecules 24:593–598

Bloomfield VA (1968) Hydrodynamic studies of structure of biological macromolecules. Science 161:1212

Broersma S (1969) Translational diffusion constant of a random coil. J Chem Phys 51:233

Budtov VP (1992) Physical chemistry of polymer solutions. Chemistry Edition, St. Petersburg

Burchard W (1961) Uber den Einfluss der losungsmittel auf die Structur linearer Makromolekule. Makromol Chem 50:20

Cantor CR, Schimmel PR (1980) Biophysical chemistry. W.H. Freeman & Company, San Francisco

Claverie JM, Dreux H, Cohen R (1975) Sedimentation of generalized systems of interacting particles. I. Solution of systems of complete Lamm equations. *Biopolymers*. 14:1685

Cowie MG, Bywater S (1965) The use of frictional coefficient to evaluate unperturbed dimensions in dilute polymer solutions. Polymer 6:197

Creeth JM, Knight CG (1965) On the estimation of the shape of macromolecules from sedimentation and viscosity measurements. Biochim Biophys Acta 102:549

Dam J, Schuck P (2004) Calculating sedimentation coefficient distributions by direct modeling of sedimentation velocity concentration profiles. Methods Enzymol 384:185

de Gennes P-G (1979) Scaling concepts in polymer physics. Cornell University Press, Ithaca

de la Torre JG, Bloomfield VA (1981) Hydrodynamic properties of complex, rigid, biological macromolecules: theory and applications. Q Rev Biophys 14:81

de la Torre JG, Jiminez A, Freire J (1982) Monte carlo calculation of hydrodynamic properties of freely jointed, freely rotating, and real polymethylene chains. Macromolecules 15:148

de la Torre JG, Martínez LM, Tirado M, Freire J (1984) Monte carlo study of hydrodynamic properties of flexible linear chains: analysis of several approximate methods. Macromolecules 17:2715

Demeler B, Saber H (1998) Determination of molecular parameters by fitting sedimentation data to finite-element solutions of the Lamm equation. Biophys J 74:444

Doi M (1996) Introduction to polymer physics. Oxford Science Publications/Clarendon Press, New York

Flory PJ (1953) Principles of polymer chemistry. Cornell Univ Press, New York

Freed KF (1983) Concentration dependence of frictional coefficient for polymer chain in solution. J Chem Phys 78:2051

Fujita H (1975) Foundations of ultracentrifugal analysis. Wiley, New York

Fujita H (1990) Polymer solutions. Elsevier, Amsterdam

Fujita H, Teramoto A, Yamashita T, Okita K, Ikeda S (1966) Solution properties of synthetic polypeptides. Sedimentation and viscosity of poly-γ-benzyl-L-glutamate in dimethylformamide. Biopolymers 4:781

Gralen N (1944) Sedimentation and diffusion measurements on cellulose and cellulose derivatives. Almqvista Wiksells, Uppsala

Gray HB, Bloomfield VA, Hearst JE (1967) Sedimentation coefficient of linear and cyclic wormlike coils with excluded-volume effects. J Chem Phys 46:1493

Harding SE, Abdelhameed AS, Morris GA (2011a) On the hydrodynamic analysis of conformation in mixed biopolymer systems. Polym Int 60:2

Harding SE, Schuck P, Abdelhameed AS, Adams G, Koek MS, Morris GA (2011b) Extended Fujita approach to the molecular weight distribution of polysaccharides and other polymeric systems. Method 54:136

Hearst JE (1964) Intrinsic viscosity of stiff-chain macromolecules. J Chem Phys 40:1506

Hearst JE, Stokmayer WH (1962) Sedimentation constants of broken chains and wormlike coils. J Chem Phys 37:1425

Hearst JE, Tagami Y (1965) Shear dependence of the intrinsic viscosity of rigid distributions of segments with cylindrical symmetry. J Chem Phys 42:4149

Imai S (1970) Concentration dependence of the sedimentation coefficient at the theta state. J Chem Phys 52:4212

Kawade Y, Watanabe I (1956) Sedimentation study of sodium deoxypentosenucleate preparations from herring sperm and calf thymus. Biochim Biophys Acta 19:513

Kinell PO, Ranby BG (1950) Ultracentrifugal Sedimentation of Polymolecular Substances. In Advances in Colloid Science 1st Ed., Eds. Mark H, Verwey EJ Vol. 3. New York : Intersci Publ: Inc. p. 161.

Kirkwood J, Riseman J (1948) The intrinsic viscosities and diffusion of flexible macromolecules in solution. J Chem Phys 16:565

Kraemers EO, Nichols JB (1940) Results obtained with svedberg ultracentrifuges. Organic colloids (Except proteins). In: Svedberg T, Pedersen KO (eds) The ultracentrifuge. Oxford University Press, New York, p 416

Kratky O, Porod G (1949) Roentgenuntersuchung gesloester Fadenmolekuele. Rec Trav Chim 68:1106

Kroe RR, Laue TM (2009) NUTS and BOLTS: applications of fluorescence-detected sedimentation. Anal Biochem 390:1

Kuhn H, Kuhn W, Silberberg A (1953) Improved relationships for diffusion and sedimentation constants and for viscosity and streaming birefringence of solutions of polymers. J Polym Sci 16:193

Landau LD, Lifschitz EM (1963) Statistical physics, 3rd edn. Pergamon Press, Oxford

Laue TM, Stafford WF III (1999) Modern application of analytical ultracentrifugation. Annu Rev Biophys Biomol Struct 28:75

Lebowitz J, Lewis MS, Schuck P (2002) Modern analytical ultracentrifugation in protein science: a tutorial review. Protein Sci 11:2067

MacGregor IK, Anderson AL, Laue TM (2004) Fluorescence detection for the XLI analytical ultracentrifuge. Biophys Chem 108:165

Maechtle W, Boerger L (2006) Analytical ultracentrifugation of polymers and nanoparticles. Springer, Berlin

Magarik SY, Pavlov GM, Fomin GA (1978) Hydrodynamic and optical properties of homologous series of styrene-methyl methacrylate graft copolymers. Macromolecules 11:294

Mandelbrot B (1982) The fractal geometry of nature. Freeman and Company, New York

Mandelkern L, Flory PJ (1952) The frictional coefficient for flexible chain molecules in dilute solution. J Chem Phys 20:212

Meyerhoff G, Appelt B (1979) A low shear viscometer with automated recording and application to high molecular weight polystyrene solutions. Macromolecules 12:968

Morris GA, Harding SE (2013) Hydrodynamic modeling of carbohydrate polymers. In: Roberts GCK (ed) Encyclopedia of biophysics. Springer, Berlin/Heidelberg

Munk P (1991) Polymer characterization using the ultracentrifuge. In: Barth HG, Mays JW (eds) Modern methods of polymer characterization. Wiley, New York

Muthukumar M, de Mense M (1983) Concentration dependent frictional coefficient of polymer molecules in dilute solution. J Chem Phys 78:2773

Newman S, Eirich F (1950) Particle shape and the concentration dependence of sedimentation and diffusion. J Colloid Sci 5:541

Oono Y (1985) Statistical physics of polymer solutions: conformation-space renormalization-group approach. Adv Chem Phys 61:301

Ortega A, de la Torre JG (2007) Equivalent radii and ratios of radii from solution properties as indicators of macromolecular conformation, shape, and flexibility. Biomacromolecules 8:2464

Ortega A, de la Torre JG (2013) Hydfit and related packages for linear molecules. In: Roberts GCK (ed) Encyclopedia of biophysics. Springer, Berlin/Heidelberg

Pavlov GM, Frenkel SY (1982) On the concentration dependence of the sedimentation coefficients of macromolecules. Vysokomol Soedin 24:178

Pavlov GM, Selunin SG, Shildiaeva NA, Yakopson SM, Efros LS (1985) Translational friction and intrinsic viscosity of polyamide benzimidazole molecules in solutions. Polym Sci USSR 27:1823

Pavlov GM, Frenkel SY (1986) Determination of the molar mass of linear polymers on the concentration dependence of sedimentation coefficient. Vysokomol Soedin 28:353

Pavlov GM, Selyunin SG (1986) Velocity sedimentation, molar mass and conformational properties of some soluble chitin derivatives. Polym Sci USSR 28:1925

Pavlov G, Frenkel S (1988) The sedimentation parameter of linear polymer molecules in absence of excluded volume effects. Acta Polymer 39:107

Pavlov GM, Panarin EF, Korneeva EV, Kurochkin EV, Baikov VE, Uschakova VN (1990) Hydrodynamic properties of polyvinylpyrrolidone molecules in dilute solutions. Makromolek Chemie 191:2889

Pavlov G.M. Korneeva E.V., Yevlampieva N.P. (1994) Hydrodynamic characteristics and equilibrium rigidity of pullulan molecules. Intern. J. Biolog. Macromolecules 16:318

Pavlov GM, Frenkel SY (1995) Sedimentation parameters of linear polymers. Progr Colloid Polym Sci 99:101

Pavlov GM, Tarabukina EB, Frenkel SY (1995) Self-sufficiency of the velocity sedimentation for the determination of the molecular characteristics of linear polymers. Polymer 36:2043

Pavlov GM (1997) The concentration dependence of sedimentation for polysaccharides. Euro Biophys J 25:385

Pavlov G, Rowe A, Harding S (1997) Conformation zoning of large molecules using the analytical ultracentrifuge. Trends Anal Chem 16:401

Pavlov GM, Harding SE, Rowe AJ (1999) Normalized scaling relations as a natural classification of linear macromolecules according to size. Prog Colloid Polym Sci 113:76

Pavlov G, Finet S, Tatarenko K, Korneeva E, Ebel C (2003) Conformation of heparin studied with macromolecular hydrodynamic methods and X-ray scattering. Euro Biophys J 32:437

Pavlov GM (2005) Normalized Kuhn-Mark-Houwink-Sakurada relationships. Polymer Sci 47A:1129

Pavlov GM, Ebel C (2006) Sedfit utilization for sedimentation coefficient determination of linear noncharged macromolecules. Abstract Book of 15th international symposium AUC, London, p 60

Pavlov GM (2007) Size and average density spectrums of macromolecules obtained from hydrodynamic data. Eur Phys J E 22:171

Pavlov GM, Amoros D, Ott C, Zaitseva II, de la Torre JG, Schubert US (2009) Hydrodynamic analysis of well-defined flexible linear macromolecules of low molar mass. Macromolecules 42:7447

Pavlov GM, Okatova OV, Michailova AV, Ulianova NN, Gavrilova II, Panarin EF (2010a) Conformational parameters of poly(N-methyl-N-vinylacetamide) molecules through the hydrodynamic characteristics studies. Macromol Biosci 10:790

Pavlov GM, Korneeva EV, Smolina NA, Schubert US (2010b) Hydrodynamic properties of cyclodextrin molecules in dilute solutions. Eur Biophys J 39:371

Pavlov GM, Perevyazko I, Okatova OV, Schubert US (2011) Conformation parameters of linear macromolecules by velocity sedimentation and other hydrodynamic methods. Methods 54:124

Pavlov GM, Breul AM, Hager MD, Schubert US (2012) Hydrodynamic and molecular study of poly(4-((4-(hexyloxy)phenyl)ethynyl)phenyl methacrylate) in dilute solutions and conformational peculiarities of brush-like macromolecules. Macromol Chem Phys 213:904

Pavlov GM (2013) Hydrodynamic of macromolecules: conformation zoning of general macromolecules. In: Roberts GCK (ed) Encyclopedia of biophysics. Springer, Berlin/Heidelberg

Pavlov GM, Okatova OV, Gubarev AS, Gavrilova II, Panarin EF (2014) Strong linear polyelectrolytes in solutions of extreme concentrations of one-one valent salt. Hydrodynamic study. Macromolecules 47:2748

Peacocke AR, Schachman HK (1954) Studies on the sedimentation behaviour of thymus deoxypentose nucleic acid with reference to its homogeneity, size and shape. Biochim Biophys Acta 15:198

Pedersen KO (1940) Results obtained with Svedberg Ultracentrifuges. Proteins. In: Svedberg T, Pedersen KO (eds) The Ultracentrifuge, Animal Proteins, Vegetable Proteins, Enzymes and Hormones, and others. Oxford University Press, New York, p 354

Perevyazko I, Vollrath A, Hornig V, Pavlov G, Schubert US (2010) Characterization of poly(methyl methacrylate) nanoparticles prepared by nanoprecipitation using analytical ultracentrifugation, dynamic light scattering, and scanning electron microscopy. J Polym Sci: Polym Chem 48:3924

Perevyazko IY, Bauer M, Pavlov GM, Hoeppener S, Schubert S, Fischer D, Schubert US (2012) Polyelectrolyte complexes of DNA and linear PEI: formation, composition and properties. Langmuir 28:16167

Peterson JM (1964) Hydrodynamic alignment of rodlike macromolecules during ultracentrifugation. J Chem Phys 40:2680

Philo JS (1994) Measuring sedimentation, diffusion, and molecular weights of small molecules by direct fitting of sedimentation velocity concentration profiles. In: Schuster T, Laue T (eds) Modem analytical ultracentrifugation. Birkhauser, Boston, p 156

Rowe AJ (1977) The concentration dependence of transport processes: a general description applicable to the sedimentation, translational diffusion, and viscosity coefficients of macromolecular solutes. Biopolymers 16:2595

Rubinstein M, Colby RH (2003) Polymer physics. Oxford University Press, New York

Sato T, Norisuye T, Fujita H (1984) Double-stranded helix of xanthan. Macromolecules 17:2696

Schachman HK (1959) Ultracentifugation in biochemistry. Academic, New York/London

Schuck P (1998) Sedimentation analysis of noninteracting and self-associating solutes using numerical solutions to the Lamm equation. Biophys J 75:1503

Schuck P (2000) Size-distribution analysis of macromolecules by sedimentation velocity ultracentrifugation and Lamm equation modeling. Biophys J 78:1606

Schuck P, Rossmanith P (2000) Determination of the sedimentation coefficient distribution by least-squares boundary modeling. Biogeosciences 54:328

Schuck P, Zhao H (eds) (2011) Modern analytical ultracentrifugation. Elsevier, Amsterdam

Schuster T, Laue T (eds) (1994) Modern analytical ultracentrifugation. Birkhauser, Boston

Scott DJ, Harding SE, Rowe AJ (2005) Analytical ultracentrifugation: techniques and methods. The Royal Society of Chemistry, Cambridge

Sharp P, Bloomfield V (1968) Intrinsic viscosity of wormlike chain with excluded-volume effects. J Chem Phys 48:2149

Singer R, Gross H (1934a) Ueber der Verhalten von Polystyrolen in der Svedberg'schen Sedimentationsgeschwindigkeits-Zentrifuge. Helv Chim Acta 17:59

Singer R, Gross H (1934b) Ultrazentrifugale Polydispersitaetbestimmungen an hochpolymeren Stoffen. Helv Chim Acta 17:726

Stafford WF (1992) Boundary analysis in sedimentation transport experiments: a procedure for obtaining sedimentation coefficient distributions using the time derivative of the concentration profile. Anal Biochem 203:295

Stafford WF (1994) Boundary analysis in sedimentation velocity experiments. Methods Enzymol 240:478

Stafford WF, Braswell EH (2004) Sedimentation velocity, multi-speed method for analyzing polydisperse solutions. Biophys Chem 108:273

Stamm AJ (1930) The state of dispersion of cellulose in cuprammonium solvent as determined by ultracentrifuge methods. J Am Chem Soc 52:3047

Stockmayer WH, Fixman M (1963) On the estimation of unperturbed dimensions from intrinsic viscosities. J Polymer Sci 1:137

Svedberg T (1927) Nobel lecture: the ultracentrifuge. http://www.nobelprize.org/nobel_prizes/chemistry/laureates/1926/svedberg-lecture.html

Svedberg T, Faehraeus R (1926) A new method for the determination of the molecular weight of the proteins. J Am Chem Soc 48:430

Svedberg T, Pedersen KO (1940) The ultracentrifuge. Oxford University Press, New York

Svedberg T, Sjoegren (1928) The molecular weight of serum albumin and of serum globulin. J Am Chem Soc 50:3318

Tanford C (1961) Physical chemistry of macromolecules. Wiley, New York

Tarabukina EB, Slavina ZN, Frenkel SY (1991) Concentration dependence of the sedimentation coefficient of poly(amidobenzimidazole). Acta Polym 42:266

Teraoka I (2002) Polymer solution: an introduction to physical properties. Wiley, New York
Tsvetkov VN (1989) Rigid-chain polymers. Plenum Press, New York
Tsvetkov VN, Klenin SI (1953) Diffusion of polystyrene fractions in dichlorethan. Dokl Akad Nauk SSSR 88:49
Tsvetkov VN, Eskin VE, Frenkel SY (1970) Structure of macromolecules in solution. Nat Lend Library Sci & Technol, Boston
Volkenshtein MV (1963) Configurational statistics of polymeric chains. Wiley, New York
Wales M, van Holde K (1954) The concentration dependence of the sedimentation constants of flexible macromolecules. J Polymer Sci 14:81
Yamakawa H (1971) Modern theory of polymer solutions. Harper & Row, New York
Yamakawa H, Fujii M (1973) Translational friction of wormlike chains. Macromolecules 6:407
Yamakawa H, Fujii M (1974) Intrinsic viscosity of wormlike chains. Determination of the shift factor. Macromolecules 7:128
Yamakawa H, Stockmayer WH (1972) Statistical mechanics of wormlike chains. Excluded volume effects. J Chem Phys 57:2843
Yanaki T, Norisuye T, Fujita H (1980) Triple helix of schizophyllum commune polysaccharide in dilute solution. Hydrodynamic properties in water. Macromolecules 13:1462
Zimm BH (1980) Chain molecule hydrodynamics by the Monte-Carlo method and the validity of the Kirkwood-Riseman approximation. Macromolecules 13:592